

W

Mobile ObserVations of Ultrafine Particles: The MOV-UP study report



The Mobile ObserVations of Ultrafine Particles (MOV-UP) study was a two-year project funded by the State of Washington to study air quality impacts of air traffic for communities located near and below the flight paths of Seattle-Tacoma International Airport. The University of Washington research team that led the study coordinated with local governments and solicited feedback from community members. A study advisory group made up of representatives from government agencies, cities and community organizations advised the study design and methods.

The material in this document may be freely used for educational or noncommercial purposes, provided that the material is accompanied by an acknowledgment line.

Authors: Elena Austin^a, Jianbang Xiang^a, Tim Gould^b, Jeffry Shirai^a, Sukyong Yun^b, Michael G. Yost^a, Timothy Larson^{ab,*} Edmund Seto^{a,*}

^a Department of Environmental & Occupational Health Sciences, University of Washington, Seattle, WA 98195, USA

^b Department of Civil & Environmental Engineering, University of Washington, Seattle, WA 98195, USA

* Co-Senior authors

Suggested citation: University of Washington Department of Environmental & Occupational Health Sciences. Mobile ObserVations of Ultrafine Particles: The MOV-UP study report. Seattle; 2019.

© 2019 University of Washington Department of Environmental & Occupational Health Sciences.



Mobile ObserVations of Ultrafine Particles: The MOV-UP study report

December 2019

Table of Contents

Executive Summary	6
Introduction	7
MOV-UP Objectives	7
Community and Stakeholder Engagement	8
About Sea-Tac Airport	10
Ultrafine Particles Description and Background	10
Methods	12
Study Design	12
Mobile Monitoring	12
Study Area	12
Mobile Monitoring Measurements	12
Fixed-site Monitoring	14
Flight and Meteorological Data	16
Instrument Calibration	16
Data Integration	17
Quality Control	17
Descriptive Statistics	17
Principal Component Analysis	18
Spatial Mapping	18
Pollutant Roses and Conditional Probability Plots	18
Fuel-Based Emission Factors	19
Results	20
Fixed-Site Sampling Results	20
Flight Data	26
Mobile Monitoring Results	27
Discussion	37
Main Study Findings	37
Uncertainties	40
Knowledge Gaps	40
Gap # 1: What are the health effects of aircraft UFP?	41
Possible Next Steps for Future Work:	41
Gap # 2: What can we do to reduce human exposures to UFP?	41
Possible Next Steps for Future Work:	41
Gap # 3: How are exposures to UFP changing over time in different communities?	42
Possible Next Steps for Future Work:	42
Bibliography	43
Appendix	47

Executive Summary

The Mobile ObserVations of Ultrafine Particles Study (MOV-UP) is a two-year project funded by Washington State to analyze potential air quality impacts of ultrafine particles from aircraft traffic for communities near and underneath Seattle-Tacoma International Airport (Sea-Tac) flight paths. The study assessed ultrafine particle concentrations (UFPs) within 10 miles of the airport in the directions of aircraft flight.

The University of Washington research team that led the study designed the project to investigate the implications of aircraft traffic at Sea-Tac by (1) assessing the concentrations of UFPs in areas surrounding and directly impacted by aircraft traffic; (2) distinguishing and comparing UFP concentrations attributable to aircraft-related and other sources and; (3) coordinating with local governments, and sharing results and soliciting feedback from community stakeholders. Over the course of four seasons, we conducted both fixed-site and mobile sampling schemes to collect time-resolved measures of UFP, carbon dioxide (CO_2), and black carbon (BC) concentrations, and UFP size distributions.

This study primarily found that UFPs derive from both roadway traffic and aircraft sources, with the highest UFP counts found nearest major roadways (Interstate 5). Total concentrations of UFP alone (10 - 1000 nm) did not distinguish roadway and aircraft features.

However, key differences exist in the particle size distribution and the black carbon concentration for roadway and aircraft features. These differences can help distinguish between the spatial impact of roadway traffic and aircraft UFP emissions using a combination of mobile monitoring and standard statistical methods.

Fixed-site monitoring confirms that aircraft landing activity is associated with a large fraction of particles in the range of 10-20 nm (ultra UFP). Mobile-derived fuel-based emissions factors (# ultra UFP/kg_{Fuel}) are consistent with differences in emissions between aircraft and roadway vehicles. The MOV-UP study findings demonstrate two clear and consistent spatial features of ultrafine particles independently associated with vehicle traffic and aircraft emissions.

We identified several knowledge gaps after analyzing this study's results. Many exist outside the scope of the initial research project but nevertheless emerge through discussion and analysis, as well as from community input and stakeholder partnerships.

See more details about the following concepts at the end of this document:

- Developing an understanding of factors (behavior, activity, emissions) that may modify human exposures to ultra UFPs.
- Developing a better understanding of the potential toxicity and health impacts from traffic- and aircraft-related UFPs.
- Characterizing how exposures to traffic- and aircraft-related UFPs change over time.

Introduction

The Mobile ObserVations of Ultrafine Particles Study (MOV-UP) is a two-year project funded by Washington State to analyze air quality from air traffic for communities near and below Seattle-Tacoma International Airport (Sea-Tac) flight paths. The study assessed ultrafine particle concentrations (UFPs) within 10 miles of the airport in the directions aircrafts fly. This study demonstrates the ability to distinguish between aircraft and other sources of UFPs, and compares UFP levels in areas impacted by high volumes of air traffic with much less impacted areas.

The research team coordinated with local governments and solicited feedback from community members. A study advisory group consisting of representatives from government agencies, cities and community organizations advised the study design and methods. We presented study progress at public meetings to obtain feedback from a broader set of aircraft-related air quality stakeholders.

WA State Proviso Sec.606.22

The State Operating Budget Proviso Sec. 606.22 for the 2017-2019 biennium funded the University of Washington School of Public Health to study the air quality implications of air traffic at the international airport in the state that has the highest total annual number of arrivals and departures, i.e., Sea-Tac.

The study must include an assessment of the concentrations of ultrafine particulate matter in areas surrounding and directly impacted by air traffic generated by the airport, including areas within ten miles of the airport in the directions of aircraft flight paths and within ten miles of the airport where public agencies operate an existing air monitoring station. The study must attempt to distinguish between aircraft and other sources of ultrafine particulate matter, and must compare concentrations of ultrafine particulate matter in areas impacted by high volumes of air traffic with concentrations of ultrafine particulate matter in areas that are not impacted by high volumes of air traffic. The university must coordinate with local governments in areas addressed by the study to share results and inclusively solicit feedback from community members. By December 1, 2019, the university must report study findings, including any gaps and uncertainties in health information associated with ultrafine particulate matter, and recommend to the legislature whether sufficient information is available to proceed with a second phase of the study.

MOV-UP Objectives

- Study the implications of air traffic at Sea-Tac.
- Assess the UFP concentrations in areas surrounding and directly impacted by air traffic.
- Distinguish and compare UFP concentrations attributable to aircraft-related and other sources.
- Coordinate with local governments and share results and solicit feedback from communities.

Community and Stakeholder Engagement

The research team coordinated with local governments, community groups and state and federal agencies throughout this two-year project to solicit feedback on the scientific design and analysis of the study, report results and take next steps. As described below, this engagement evolved over time and inspired many stakeholders to participate actively in the program. We will continue to consult with these stakeholders and remain engaged as we disseminate the results from this project through factsheets, press releases and public presentations.

External Advisory Group

The Dean of the University of Washington School of Public Health established an external advisory group to provide important feedback to the research team on every phase of the study, including: (1) Defining primary objectives; (2) Feedback on sampling methods and plans; (3) Feedback on results and interpretation and; (4) Priority knowledge gaps this process identifies. The advisory group also provided final comments on the content of this report as well as dissemination ideas and opportunities. This advisory group included representatives from the following organizations:

MOV-UP Study Advisory Group

- Beth Friedman, WA State Department of Ecology
- Brandon Miles, City of Tukwila
- Bonnie Wilkins, City of Des Moines
- Clark Halvorson, WA State Department of Health
- Courtney Gregoire, Port of Seattle
- Darrell Rodgers, Public Health - Seattle & King County
- Debi Wagner, City of Burien
- Jaime Rossman, WA State Department of Commerce
- John Resing, Quiet and Healthy Skies Task Force
- Julie Fox, WA State Department of Health
- Karl Pepple, US EPA Region 10
- Kathy Strange, Puget Sound Clean Air Agency
- Katie Skipper, WA State Department of Ecology
- Leslie Lardie, FAA Northwest Mountain Region
- Mark Hoppen, City of Normandy Park
- Michael Matthias, City of Des Moines
- Office of Congresswoman Pramila Jayapal, WA State 7 th Congressional District
- Office of Congressman Adam Smith, WA State 9th Congressional District
- Office of Representative Mike Pellicciotti, WA State 30th Legislative District
- Office of Representative Tina Orwall, WA State 33rd Legislative District
- Peter Kwon, City of SeaTac
- Ralph Iovinelli, FAA
- Roseanne Lorenzana, Beacon Hill Community Noise Team & Quieter Skies Task Force
- Shirlee Tan, King County Department of Public Health, Environmental Health Services Division
- Stephanie Meyn, Port of Seattle
- Veronica Valdez, Port of Seattle

The views expressed in this report do not necessarily reflect the official policies of the individuals, agencies, departments and organizations serving on this project's Advisory Group. The authors would like to thank all of the Advisory Group members and their designees for their time, dedication, support and valuable comments and suggestions.

Presentations to the external advisory group

Presentations to the external advisory group included an initial introductory meeting (January 5th, 2018), a mid-project update (August 15th, 2018), and a final presentation of results (September 4th, 2019). At the introductory meeting we invited members to comment on the location of mobile monitoring routes and to propose fixed-site sampling locations described in the methods below. Input from this discussion allowed researchers to finalize the mobile monitoring routes and identify and facilitate access to fixed-site sampling sites. At the mid-project update, we presented participants with initial analysis approach based on two seasons of data collection. The advisory members provided direct feedback on the approach. Additionally, the advisory group considered the following steps forward proposed by the research team:

- Impact of time-of-day on ultrafine distributions (73% of participants identified this as a high/urgent priority);
- Impact of meteorology on flight patterns and pollutant measures (50% identified this as a high/urgent priority);
- Importance of relating flight traffic to ultrafine PM measurements (93% of participants identified this as high/urgent priority);
- Desirability of incorporating SO₂ measures in data collection (80% of participants identified this as a high/urgent priority).

As a direct result of these discussions, the research group obtained the 2018 flight path data from the Federal Aviation Administration (FAA), incorporated 15-minute Washington Automated Surface Observing System (ASOS) Network weather data into the analysis and also considered hour of day. Unfortunately, the MOV-UP researchers could not secure an appropriate SO₂ measurement instrument.

The final advisory meeting allowed the research group to generate discussion about interpreting study findings, best opportunities for disseminating findings and develop consensus on important knowledge gaps and next steps. Participants provided some feedback on graphical representations of data in figures and charts.

Presentations and engagement with community

In addition to the external advisory group, senior UW scientists made frequent appearances at the Highline Forum. The Highline Forum provides Southwest King County municipalities, educational governing bodies and the Port of Seattle with the opportunity to share information, interact with outside speakers and other governmental organizations and work in partnership on initiatives that benefit the residents of Southwest King County. These meetings included both formal presentations by researchers as well as informal discussion and feedback sessions.

Presentations to the Highline Forum

- November 2017: Background information on UFP and introduction to the study objectives.
- March 2018: Update on study design and methods.
- January 2019: Study progress and preliminary results.

Presentations to local, state and federal agencies

The research group also engaged with several agencies and delivered presentations to government agencies to engage and solicit feedback from partners, including:

- Public Health – Seattle & King County (February 2019): Presentation of initial results and analysis approach.
- Federal Way Council (April 2019): A public meeting held at Federal Way Council Meeting to provide an update on the MOV-UP study and ideas for a longer-term UFP monitoring network.

- FAA AEC Roadmap Meeting (May 2019): An invited presentation with FAA to present progress on the MOV-UP study.
- Airport Impact Study SeaTac City Hall (May 2019): An update on the MOV-UP study at a SeaTac City Hall public meeting related to the Airport Impact Study.
- Port of Seattle update (July 2019): An update on the MOV-UP study for Port of Seattle representatives.

Communication Plan

We created a website (<https://deohs.washington.edu/mov-up>) at the project's launch. The website includes a short description of the research project, a project timeline and a description of the External Advisory Group. Throughout the project we have updated the website with all materials from presentations for the public and at government agencies. In addition, we provide contact information for key individuals. We also periodically update the project website with media coverage we receive.

Members of the project advisory group received a draft of the final report in October 2019. This document incorporates their comments and suggestions. The UW research group is solely responsible for the final content and interpretation of study results. Therefore, this report does not necessarily reflect the official policy or position of any of the stakeholder groups.

About Sea-Tac Airport

Sea-Tac is the 8th busiest US airport by passenger boarding, and the busiest airport in the state of Washington. In 2018, Sea-Tac transported more than 49.8 million passengers and greater than 430,000 metric tons of air cargo.¹ Sea-Tac operates in a south-flow or north-flow condition, depending on the direction of prevailing winds. Aircraft fly into winds from the south, and arrive from the north. This pattern occurs most commonly during the cooler, cloudier months of the year characterized by low-pressure systems and on-shore flow. The airport conducts south-flow operations approximately 65% of the year. When winds blow from the north, aircraft depart the airport in that direction and arrive from the south, occurring most commonly during warmer, high-pressure, clear periods of the year.

Ultrafine Particles Description and Background

UFPs are defined in this study as particles with a diameter of less than 100 nanometers (nm), consistent with the definition proposed by the US EPA². Sources of UFPs in ambient air include combustion processes and secondary aerosols formed through atmospheric chemistry reactions. Very complex spatial distributions of UFPs have been associated with urban environments, typically relating to strong gradients in concentrations on and near roadways and other major sources, including residential wood burning, industrial sources and photochemical transformation of gaseous pollutants. Elevated concentrations of UFPs have been reported near and on freeways and near to airports.³⁻⁷ An important aim of this study is to develop methodology to distinguish between UFPs from roadway traffic and those from aircraft.

Typical reported urban background concentrations of ultrafine particles range from 5,000-40,000 particles/cubic centimeter⁸⁻¹⁶ (often abbreviated as #/cm³); typically, weather and proximity to roadways and airports impact background concentrations. Because these particles are so tiny, even when many particles are present, the total mass associated with these particles is typically less than 2 micrograms per cubic meter (µg/m³) and UFP is not considered an important contributor to the mass concentration of PM_{2.5}, particles with diameter less than 2.5 micrometers (µm), which is the regulated form of particulate matter.

Therefore, UFPs are usually not collected and weighed as PM_{2.5} concentrations are often quantified, but rather counted in real-time using instruments, such as a condensation particle counter (CPC). The CPC condenses liquid on the surface of individual particles so that they grow to sufficient size for a laser to detect and count them. Because UFPs are counted, the unit of concentration is therefore a particle number concentration (PNC), i.e., #/cm³ rather than µg/m³.

The health effects associated with PM_{2.5} mass concentrations have been well studied, and this has led to established standards and routine monitoring.² However, PM_{2.5} consists of a mixture of particles of varying sizes from a variety of sources, with the most numerous particles by count usually falling within the ultrafine size range <100 nm. In the ambient environment, the spatial and temporal variation of UFPs tends to differ from PM_{2.5} or PM₁₀,¹⁷ and we understand much less about the health effects of UFP.¹⁸

Early toxicological studies suggested that UFP may be more relevant to health than larger-sized particles due to the larger surface area relative to mass of UFPs, and the ability for smaller sized particles to penetrate within the body.^{19, 20} While the epidemiologic evidence for UFP health effects is still limited, there exists sufficient studies to inform quantitative concentration-response functions for all-cause mortality,¹⁸ and recent large epidemiologic studies have considered UFP exposure estimates for a variety of outcomes, including breast cancer,²¹ ischemic heart disease,²²⁻²⁶ prostate cancer²⁷ and asthma and COPD.²⁸

Although much of the previous research on environmental variations in UFP concentrations has focused on roadway vehicle emissions of UFPs,²⁹⁻³⁶ recent research identifies a previously under-appreciated source of UFP, which may be responsible for large population exposures globally. Monitoring campaigns conducted in communities near the Los Angeles,^{3, 4, 37} Atlanta,³⁸ Boston,^{5, 6} New York³⁹ and Amsterdam⁷ airports have all identified elevated levels of UFP attributable to aircraft flight emissions. In the study at Los Angeles LAX, on which our study team collaborated, we observed UFP levels four times higher than background levels—even 10 km (6.2 mi) away from the airport. The study highlighted a new concern for communities near major airports, where many more people may be exposed to UFPs from aircraft compared to roadway exposures.

Few epidemiologic studies assess the associations between aircraft UFP exposures and health. One limited study of two specific locations in Los Angeles observed that short-term exposure to aircraft-related UFP is associated with elevated systemic inflammation (IL-6); whereas, roadway traffic is more associated with impaired respiratory health (lower FEV₁) and inflammation (elevated sTNFrlI). This suggests that the short-term effects of aircraft-related UFP exposure may be distinct from roadway traffic UFP exposure.⁴⁰

It was noted in this study that in order to estimate health effects and accurately assess exposures it is necessary to consider the entire source to receptor pathway, starting from emissions, composition, fate and transport, exposures and confounding factors in the population of interest. The authors also suggested that replicating these findings requires further work.

The WA State Department of Health is conducting a literature review of UFP health impacts. A report of their review should be available by the time our final report is published (Summary of health research on ultrafine particles. Office of Environmental Public Health Sciences, Washington State Department of Health, November 2019).

Methods

Study Design

We conducted sampling for the MOV-UP study seasonally from February 2018 through March 2019, using two primary sampling designs. The first—a mobile sampling design with two hybrid-electric vehicles equipped with sampling instruments and an isokinetic probe—sampled ambient air as the vehicles moved through defined routes. A traffic-related air pollution study used this same strategy and its results demonstrated the validity of on-road measurement in detecting pollutant gradients and important emissions characteristics.³² In addition, we also used a fixed-site sampling scheme to characterize 24-hour air pollutant characteristics near roadway, near airport and in background sites.

Mobile Monitoring

Study Area

This study assesses UFP concentrations near the airport in the directions of aircraft flight; it attempts to distinguish between aircraft and other sources of UFPs by comparing levels of UFPs in areas impacted by high volumes of air traffic with those that are much less impacted. Mobile monitoring occurred along defined routes that we termed transects, which were designed to sample in an east-west direction at fixed latitudes north and south of the airport.

Because of terrain and roadway considerations, some transects deviated slightly from the target latitude. We monitored transects 10 miles north (five transects) and 10 miles south (six transects) of the airport. We designed this campaign to capture multiple repeated samples of each transect (Figure 1). Please see a summary description of each route in the appendix.

We kept the time of day to afternoon to increase comparability between the different sampling repeats and to minimize the effect of a changing height of the atmospheric mixing layer. In the interest of decreasing confounding by weather patterns and other time-varying changes in UFP concentration, many sampling days consisted of two simultaneous sampling vehicles north and south of the airport.

Mobile Monitoring Measurements

A detailed description of the mobile platform is given elsewhere.^{36, 41} In summary, each mobile monitoring platform consisted of a Toyota Prius hybrid-electric vehicle from University of Washington Fleet Services and several portable monitors for air pollution measurements.

We mounted a GPS logger on the dash of the vehicle to record its position and speed, and mounted a sampling inlet on the roof of the vehicle pointing forward. The sampling inlet was positioned above the vehicle boundary layer, the zone of turbulence directly associated with vehicle motion, and connecting tubes entered the vehicle through the otherwise sealed left rear window from where they were connected to the instruments.

Figure 1: Mobile ObserVations of Ultrafine Particles (MOV-UP) Study Setup.

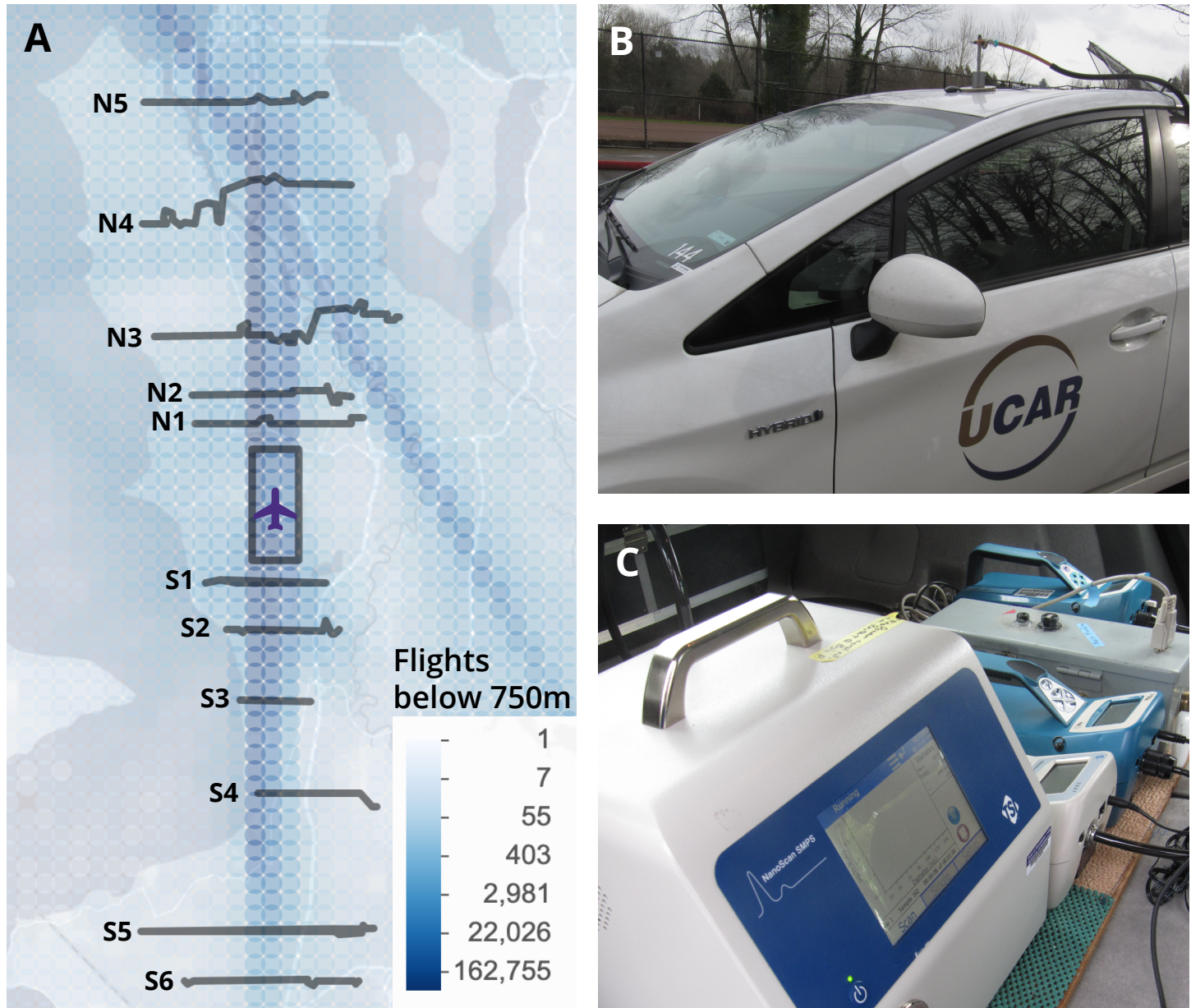


Figure 1. A. Displayed on the map are the location of the five transects North of the airport, labeled N1-N5, and the six transects South of the airport, labeled S1-S6. In blue, the density of flights at an altitude of 750m or less is overlaid on the street map. B. Mobile platform with rooftop air inlet. C. Sampling manifold and monitoring instruments.

Particle loss was minimized by using stainless steel, copper, and conductive flexible tubing for the particle sampling inlet and connecting tubing. The exhaust pipe from the vehicle's gasoline engine discharged on the right side low to the ground, away from the elevated, left-side air monitoring inlet. To further minimize the potential for self-pollution, the vehicle's gasoline engine would typically shut off when stopped at red traffic lights.

Throughout the campaign, each platform was equipped with a CPC (Model 3007, TSI Inc., MN), two P-Trak (Model 8525, TSI Inc., MN) condensation nuclei particle counters (one with inlet diffusion screens to increase the minimum detected particle size), a black carbon aerosol monitor (microAeth AE51, AethLabs, CA), a CO₂ analyzer (Li-850, LI-COR, NE), and a GPS Receiver (DG-500, GlobalSat WorldCom Corporation, TW). Additionally, a NanoScan SMPS Nanoparticle Sizer (Model 3910, TSI Inc., MN) was rotated in the two platforms. All these instruments except the NanoScan measured and recorded data at one-second intervals.

The CPC and the P-Trak measured the total number concentrations of particles larger than 10 nm diameter and 20 nm diameter, respectively; while the P-Trak with the inlet diffusion screen used in this study measured the total number concentrations of particles larger than 36 nm diameter. The NanoScan measured during a 1-minute interval nanoparticle size distributions with 13 bins measuring 10 to 420 nm.

The microAeth AE51 quantifies black carbon (BC) from the amount of light absorbed by sampled particulate matter and application of an extinction parameter to convert optical attenuation into a BC mass concentration. The Li-850 CO₂ analyzer monitored CO₂ concentration based on non-dispersive infrared (NDIR) techniques. The GPS Receiver measured the position (longitude, latitude and elevation) and speed of each vehicle with an accuracy of ± 5 m.

Table 1: Summary of instruments used in the MOV-UP Study

Parameter (units)	Instrument	Manufacturer	Accuracy
≥10nm Particle Count (#/cm ³)	CPC 3007	TSI	N/A
≥20nm Particle Count (#/cm ³)	P-Trak 8525	TSI	N/A
≥36nm Particle Count (#/cm ³)	P-Trak 8525 with 36 nm diffusion screen	TSI	N/A
10-420nm Nanoparticle Size Distributions (#/cm ³)	NanoScan 3910	TSI	N/A
BC (ng/m ³)	AE51	AethLabs	±100 ng BC/m ³
CO ₂ (ppm)	Li-850	LI-COR	<1.5%
Location and Speed	GPS Receiver DG-500	GlobalSat	Position: <2.5m Velocity: 0.1m/s

Fixed-site Monitoring

Note the locations and sampling duration at the fixed-site locations in Figure 2 and Table 2, respectively. We monitored sites across seasons for periods of one or two weeks, with two different sampling manifolds. The sampling locations by season are presented in Table 2.

Throughout the fixed-site monitoring, we equipped each sampling location with a CPC (Model 3007, TSI Inc., MN), two P-Trak (Model 8525, TSI Inc., MN) condensation nuclei particle counters (one with an inlet diffusion screen), a black carbon aerosol monitor (microAeth AE51, AethLabs, CA), and a CO₂ analyzer (Li-850, LI-COR, NE). We deployed a NanoScan SMPS Nanoparticle Sizer (Model 3910, TSI Inc., MN) at one monitoring fixed site.

Figure 2: Four fixed-site monitoring locations.

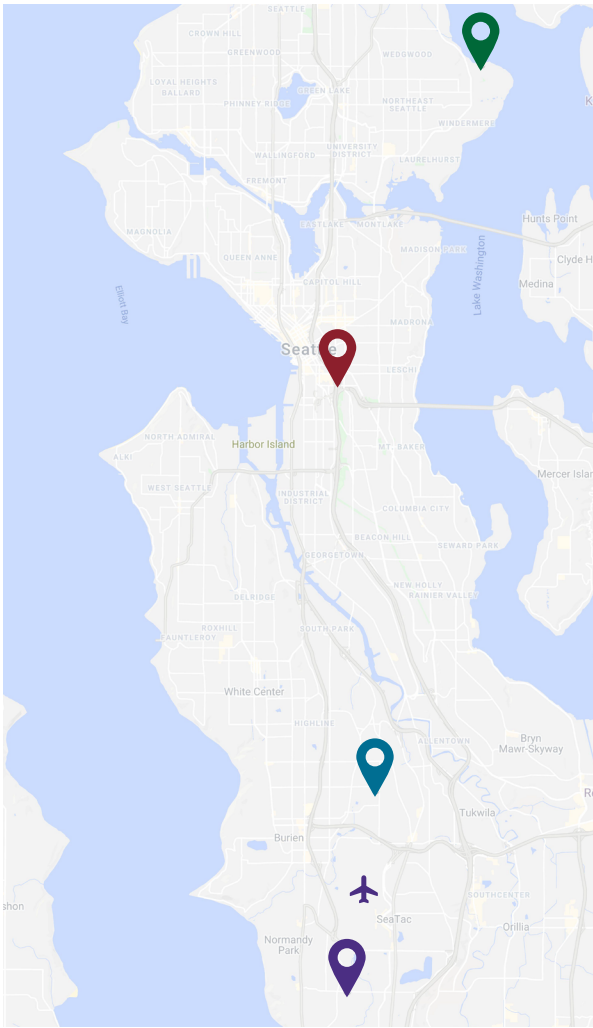


Table 2: Fixed-site monitoring sampling periods and proximity to aircraft traffic.

	Urban Background	Near Highway	North of Airport	South of Airport
Season	Sampling Days	Sampling Days	Sampling Days	Sampling Days
Spring	23	8	0	10
Summer	13	0	11	13
Fall	0	0	16	15
Winter	0	0	8	7

	Urban Background	Near Highway	North of Airport	South of Airport
Overhead Flights*	75	2,014	46,799	127,202

*Overhead Flights: Refers to the number of flights flying within approximately 600 m (horizontally) of the monitoring location and below a vertical altitude of 750 m in 2018. We chose 750 m as a vertical altitude cap because this generally represents the upper limit of the atmospheric boundary layer height. We chose not to present this by sampling season because of some missing aircraft track data from Winter 2019.

All these instruments, except the NanoScan, measured and recorded data at 10-second intervals. The NanoScan scanned and recorded data across all size bins every 60 seconds. See the description of the mobile monitoring platform for details on the operation and parameters each instrument measured.

Flight and Meteorological Data

We requested flight data from the FAA western regional office using a data-disclosure request. The data covered 2018 and included track data for all the flights in the Seattle metropolitan region. We gridded the density of flights with an altitude of less than 750 m in cells of 70x100 m by hour of the year for the study domain. We used single aircraft track data to calculate predominant landing direction as well as number of flights landing per hour. The flight data included flights arriving and departing from all local airports.

The Washington Automated Surface Observing System (ASOS) Network⁴² provided us with wind speed and direction, temperature and relative humidity based on 15-minute data from Sea-Tac.

Instrument Calibration

All instruments were calibrated for flow, zero and span in the factory before we received them. The Li-850 CO₂ analyzer was calibrated for zero and span in the lab with certified standard CO₂ gas. We conducted mobile co-location calibration with all sets of UFP and/or BC monitors deployed in one vehicle. Since there are no traceable standards for calibration of UFP and BC monitors, we used the averaged measured results of all sets of duplicate monitors as the reference. See Table 3 for the summary of calibration coefficients and R². Note that five P-Trak monitors, four P-Trak screened monitors, two CPC monitors and three AE51 monitors were rotated in the two vehicles. Thus, the calibration results include all those monitors.

Table 3: Summary of co-location calibration results for PNC and BC monitors.

Instrument	Intercept*	Slope	R ²
P-Trak 1#	539	0.93	0.990
P-Trak 2#	197	0.97	0.992
P-Trak 3#	-941	1.28	0.992
P-Trak 4#	213	0.95	0.999
P-Trak 5#	127	0.90	0.974
P-Trak screened 1#	386	0.87	0.966
P-Trak screened 2#	372	1.04	0.955
P-Trak screened 3#	673	1.05	0.948
P-Trak screened 4#	673	0.89	0.987
CPC 1#	1208	1.20	0.993
CPC 2#	-647	0.85	0.996
AE51 1#	16	0.98	0.791
AE51 2#	143	0.89	0.932
AE51 3#	37	1.00	0.964

* Intercept units: #/ cm³ for PNC monitors, and ng/m³ for BC monitors.

Data Integration

At the end of each sampling day we collected raw data from each instrument on a secure server. We developed a merging script to:

- Compute a 30-second center-aligned rolling means to smooth concentrations of CO₂ and one-second particle numbers.
- Smooth the BC data using an Optimized Noise-reduction Averaging (ONA) algorithm (with attenuation coefficient (ATN) threshold set to ΔATN = 0.06) to reduce potential instrumental optical and electronic noise.⁴³
- Apply a common one-minute time basis for all sampling instruments. Instruments that sampled on a one-second basis were averaged to longer intervals;
- Calculate short-term 30-minute background concentrations for black carbon and particle count, based on the method presented elsewhere.³²
- Apply between-instrument calibration factors as discussed in the “Quality Control” section.
- Merge meteorological parameters and flight data per one-hour metric. We averaged one-minute pollutant data over longer intervals.

Quality Control

We also performed data quality control and applied the following criteria:

- We excluded GPS coordinates from the analysis that were outside of the study zone presented in Figure 1.
- We flagged as erroneous total particle concentration of less than 100 #/cm³ measured from CPCs and NanoScan.
- We excluded values of black carbon from the data exceeding 27,000 ng/m³ (0.01% of the data).
- We based one of our particle metrics between 10 nm and 20 nm on the difference in short-term measures of the CPC and P-trak instruments. In instances where this difference was negative (< 1.2% of the collected data), we replaced the negative value with a random normal distribution of data centered around one particle/cm³, eliminating negative values in the data.
- Automated flagging routines censored data corresponding to instrument error codes, instruments operating out of specified parameters or data otherwise missing (instrument rebooted itself, lost power, etc.). We then manually inspected the time series for each pollutant for anomalies and cross checked with field technician notes.

We combined the resulting fixed-site and mobile monitoring data into a final data analysis data file, and performed all data management in R version 3.5.1, which is reproducible.

Descriptive Statistics

We computed descriptive statistics of the collected data including mean, median, interquartile range and range, and performed graphical representation of the data using the ggplot2 library in R. We performed post-hoc comparison of concentrations between fixed-sites using a Mann-Whitney test on the paired data.

We calculated some informative pollutant ratios for descriptive purposes on account of the prevalence of various particle sizes and contribution of black carbon soot originating from different emission source types, including the:

- Proportion of 10-20 nm particles relative to total measured particles.
- Proportion of 20-36 nm particles relative to total measured particles.
- Proportion of 10-20 nm particles to black carbon concentration.

We calculated the concentration of particles above the background concentration of total particles as the quantity above the 5th percentile of the 30-minute concentration of particles. This approach has been successfully employed in previous mobile monitoring campaigns to account for neighborhood-level concentrations.^{31, 38}

Principal Component Analysis

We performed principal component analyses (PCA) on the mobile monitoring data using the psych and GPA rotation packages in R. We retained factors with eigenvalues greater than 1 and applied a Varimax rotation to the PCA results to improve factor interpretability.

We developed input variables beyond the directly measured variables to the PCA analysis in order to capture a variety of composition and size information on the particles collected over the mobile monitoring campaign. We calculated a primary PCA solution using variables obtained from the full data set of mobile monitoring, and we calculated a second PCA based on a subset of data that included particle size distribution information from the NanoScan instrument.

We developed the second PCA solution in order to help interpret and validate the full model. We compared results of the two PCA analyses using both correlation of the scores as well as composition information. We interpreted principal component features and spatially linked them using the GPS data collected during the mobile monitoring drives. We predicted PCA components at the fixed sites using the initial model developed from the mobile monitoring data. And, we standardized scores to the values from the initial mobile monitoring dataset.

Spatial Mapping

We performed mapping of pollutant, principal component and flight patterns on a grid of 0.001 degrees of longitude (~70 m) and 0.002 degrees of latitude (100 m). We represented the distribution of pollutant concentrations on a quantile scale, and performed plotting using the R implementation of the leaflet JavaScript tool.

Pollutant Roses and Conditional Probability Plots

We used ASOS weather data collected every 15 minutes at Sea-Tac Airport to develop pollutant roses and conditional probability plots at the fixed-site locations north and south of the airport. The pollution rose classifies the collected pollutant data for each site based on the direction of the wind, allowing for the suggestion of the geographical direction of plumes affecting the site.

Conditional probability plots further refine this analysis by identifying the probability that a given wind direction and wind speed is associated with a high concentration of pollutant. For our analysis, we used a threshold of 90th percentile of the measured data to define “high concentrations.” Conditional probabilities are scaled between 0 and 1 where 0 represents 0% probability that a given wind direction and speed is associated with a high concentration and 1 represents 100% probability that a given wind direction and wind speed is associated with a high concentration. We plotted the results of the conditional probability analysis on a polar plot

where the spokes represent wind direction, the concentric circles wind speed and the colors the conditional probabilities. We performed analyses using the openair package in R.

Fuel-Based Emission Factors

Fuel-based emissions factors are typically computed as a concentration of emissions produced per gram of fuel burned. The emission factor of particular interest in this study is the very smallest range of UFP that we termed “ultra-ultrafine particles” (Ultra-UF), defined by the following numeric factor:

$$\text{Emission Factor (EF)} = \frac{\text{\# of Ultra-UF Particles (10-20 nm)}}{\text{Fuel (g)}}$$

We do not know the total grams of fuel burned for the traffic and aircraft sources. However, we can use the change in measured ambient CO₂ concentration over a short time period as a proxy for changes in fuel consumption. The change in CO₂ relates to fuel consumptions by estimating the weight fraction of carbon (ω_c) in the traffic and aircraft fuel. We reported these weights in the literature measuring between 0.85-0.87 for traffic and 0.86 for Jet A fuel.⁴⁴

Based on a method described by Shirmohammadi et al.,⁴⁵ we estimated the fuel-based emissions factors for quantiles of locations we identified as “high aircraft impact” and “high traffic impact” through the PCA analysis. We estimated urban background concentrations as the 5th percentile of the data collected during each hour of monitoring,²⁶ for both the Ultra-UF and CO₂ concentrations. We performed calculations as:

$$EF_p = \left(\frac{[P]_i - [P]_{bg}}{[CO_2]_i - [CO_2]_{bg}} \right) \omega_c \times \alpha$$

Where,

- [P]_i represents the concentration of UltraUF particles at the impact area (#/cm³)
- [P]_{bg} represents the hourly background concentration of UltraUF particles (#/cm³)
- [CO₂]_i represents the concentration of CO₂ at the impact area (g/m³)
- [CO₂]_{bg} represents the hourly background concentration of CO₂ (g/m³)
- ω_c is the weight fraction of traffic and aircraft fuel
- α is the unit conversion factor (10¹²)

Results

Fixed-Site Sampling Results

Fixed-site results revealed seasonal differences and between-site differences in pollutant concentrations (Figure 3, Figure 4, Figure 5). We observed the highest concentrations of total UFP (particles between the sizes 10-1000 nm) at the near-highway site next to Interstate 5, followed by the site south of the airport along S. 200th St.; these sites also had higher variability overall.

There were significantly lower concentrations of traffic-related pollutants and CO₂ at the urban background site (Figure 6). We statistically tested differences between the south of airport and north of airport sites using a pairwise Wilcoxon Rank Test. There were significant differences in all the pollutants measured ($p < 0.001$) across all seasons and pollutants (Figure 3, Figure 4, Figure 5).

Figure 3: Total particle concentration at the fixed-site locations by season.

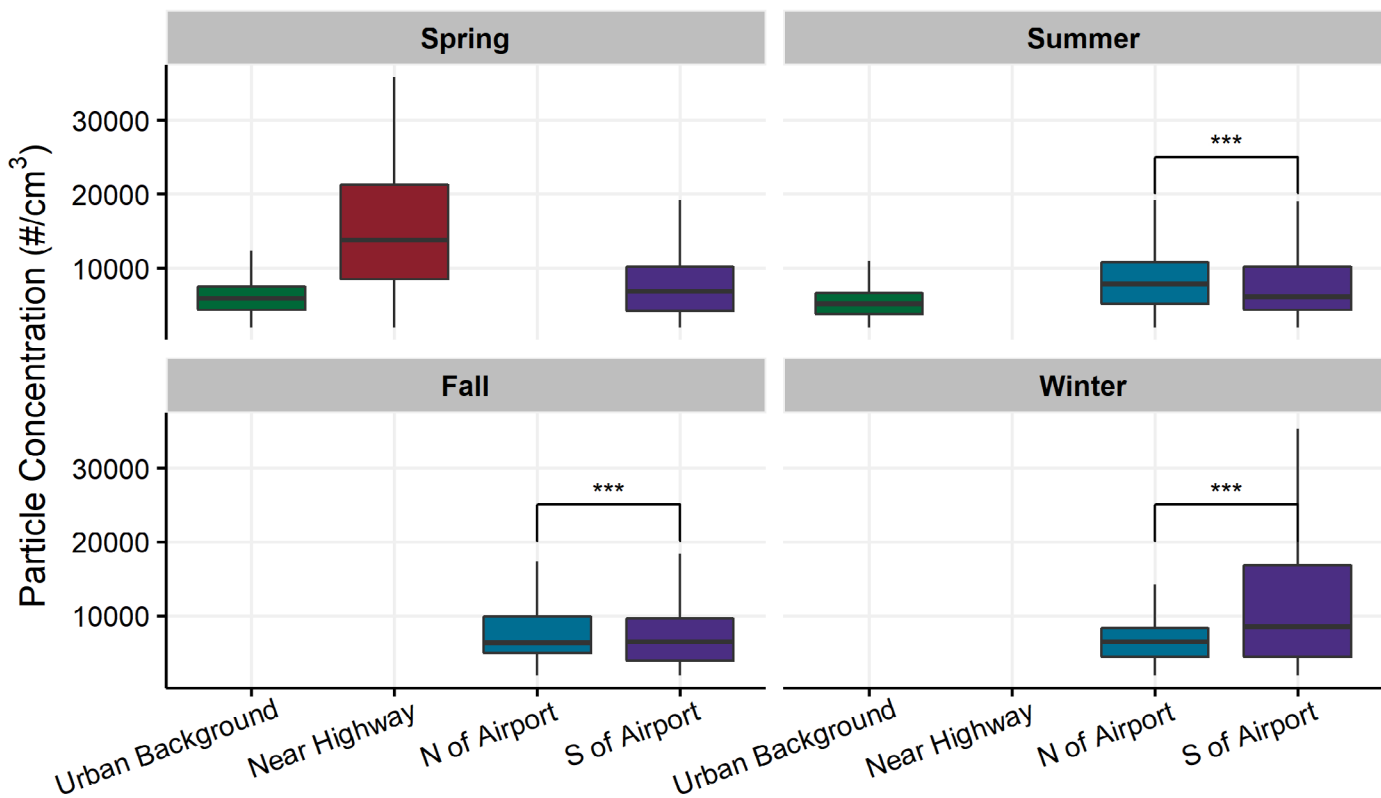


Figure 3. The total particle concentration is the total count of particles between 10 and 1000 nm in diameter in a cubic centimeter of air.

Figure 4: Black carbon concentrations at the fixed-site locations by season.

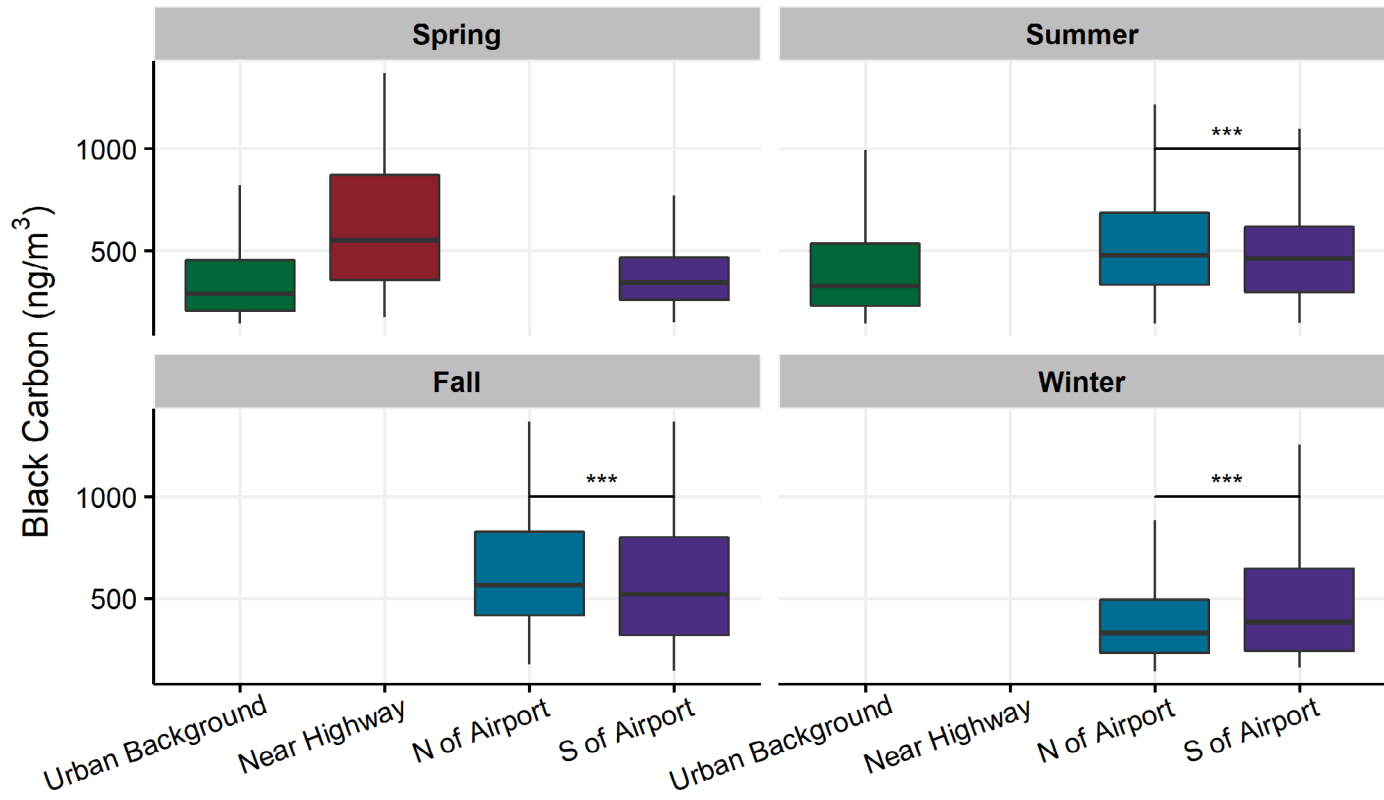


Figure 5: Carbon dioxide concentrations at the fixed-site locations by season

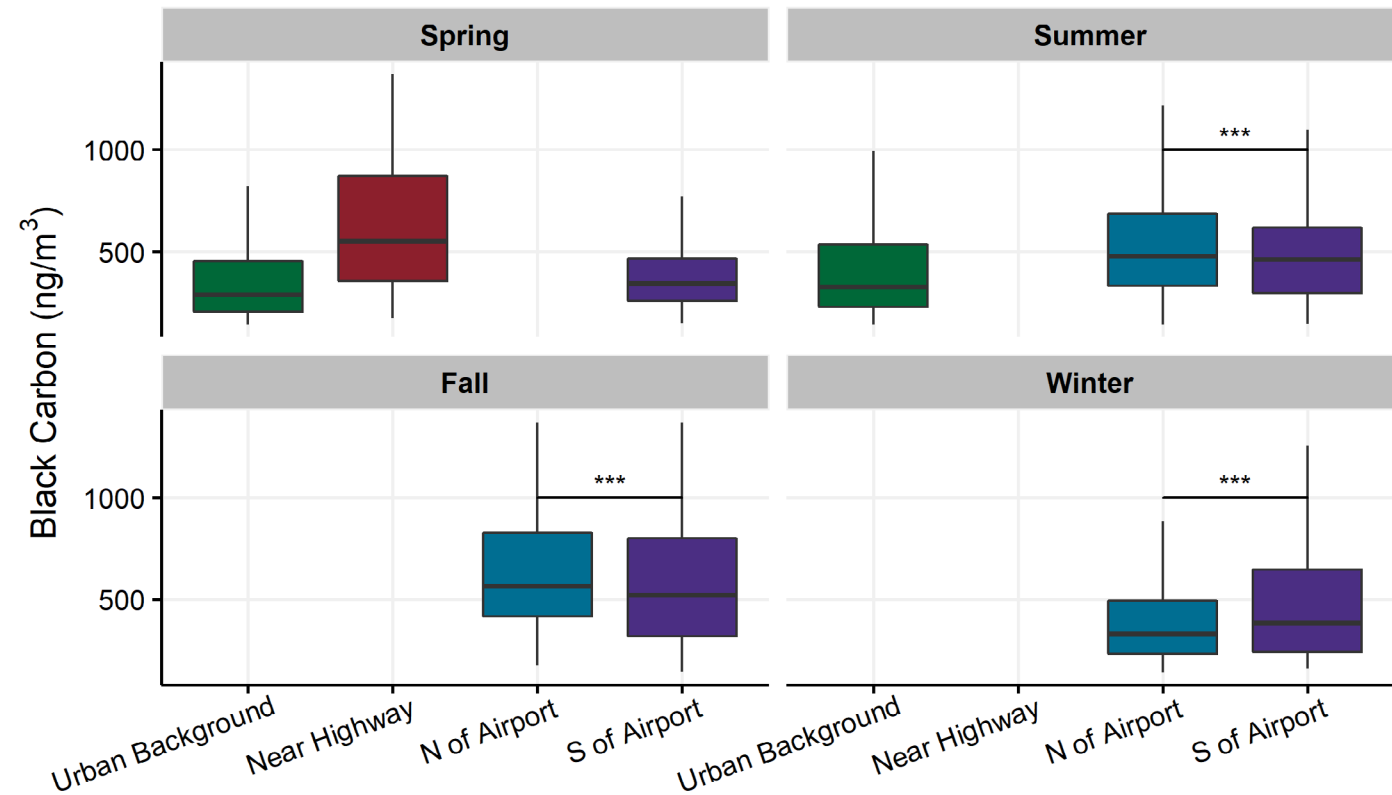


Figure 6: Overall comparison of traffic-related pollutants at the fixed sampling sites.

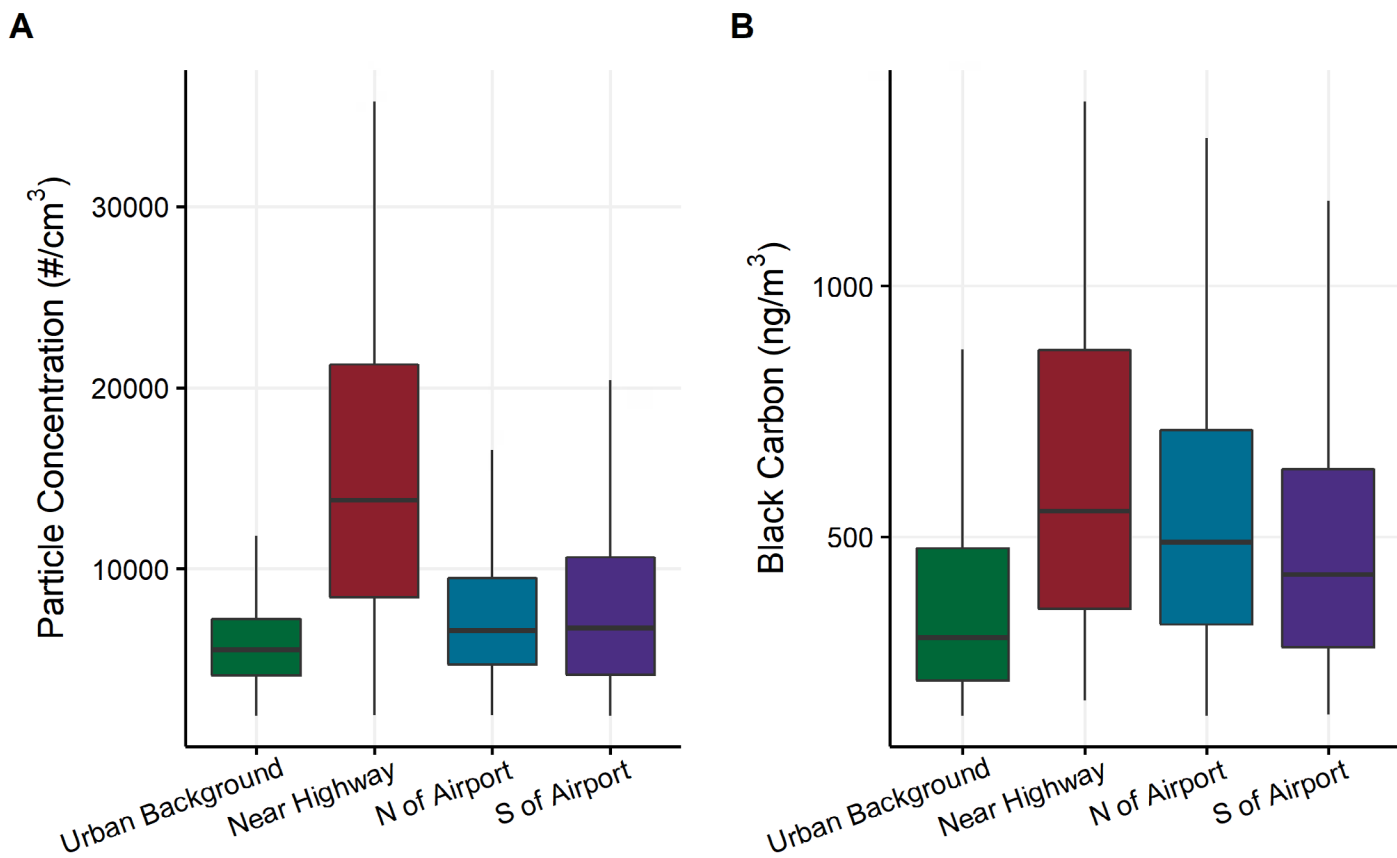
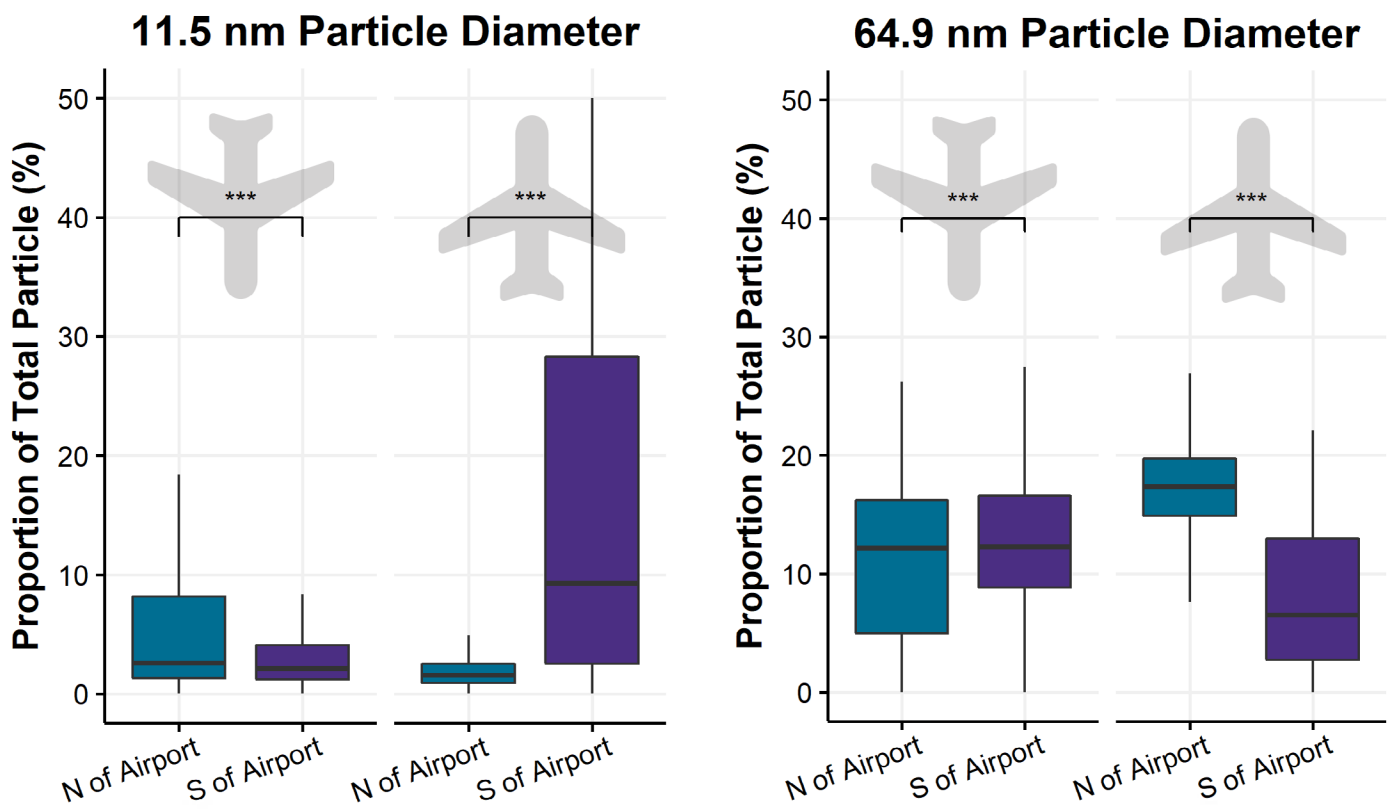


Figure 6 - A. Total particle (>10 nm) number. B. Black carbon concentration.

We examined the proportion of ultra-UFP (the ratio of particles 11 nm in diameter to Total UFP from the NanoScan) and the proportion of mid-size UFP (the ratio of particles 65 nm in diameter to Total UFP from the NanoScan) at the fixed-site locations north and south of the airport. These proportions range from 0 to 1 where 0 represents none of the measured UFPs were of the diameter of interest, and 1 represents cases where all the measured particles were of relevant diameter.

We divided the observation period by the hourly landing direction of the aircrafts. In total, we sampled 402 hours of aircrafts landing overhead and 437 hours of aircrafts ascending overhead. Figure 7 demonstrates a significant increase in ultra-UFP fractions related to times when aircraft are landing overhead. The proportion of larger 65 nm particles do not show a significant change associated with the landing of aircrafts over the sampling location.

Figure 7: Distribution of ultrafine particles as a proportion of the total particles when aircraft are flying overhead.

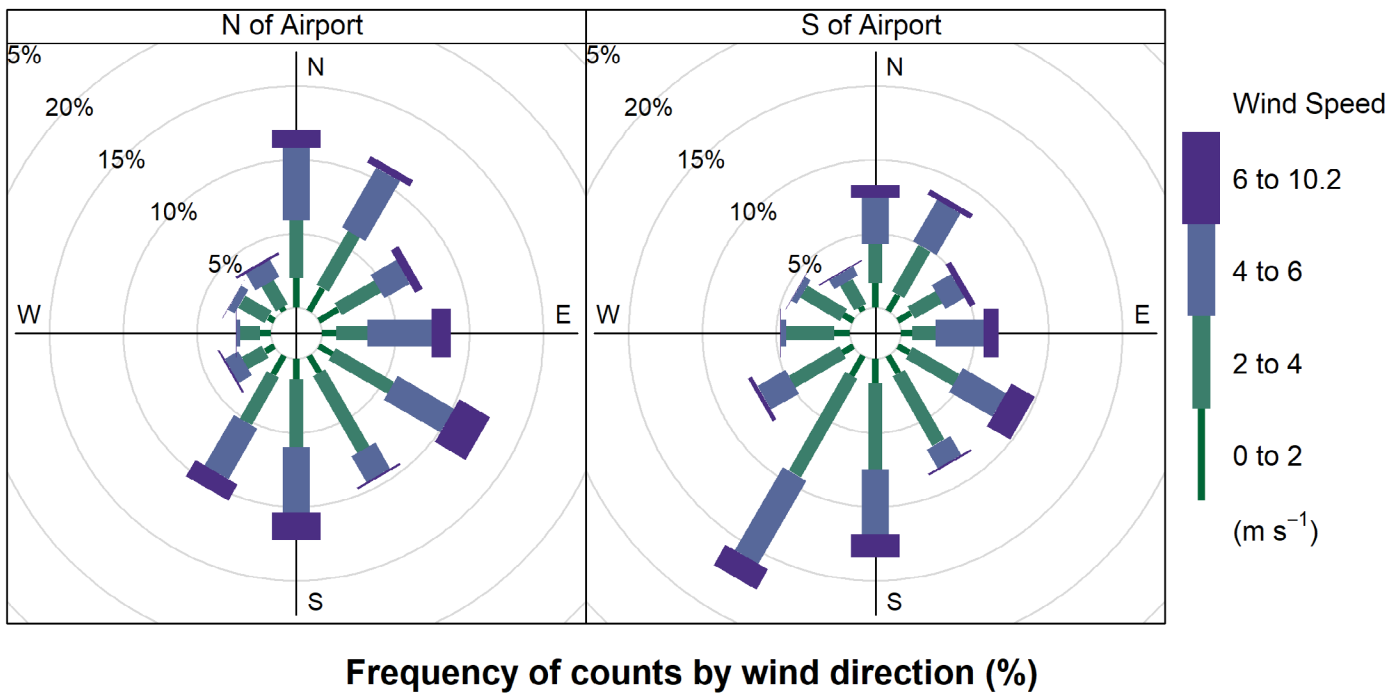


We examined the wind roses and pollutant roses associated with Total Particle Concentration (#/cm³) observed during the fixed-site sampling north and south of Sea-Tac. These results, presented in Figure 8, indicate that the highest quintile of Total Particle Concentrations (> 17,000 #/cm³) were associated with time periods when the wind blew from the airport's direction with respect to the sampling site. These data indicate that the distribution of pollutant concentrations does not correspond to the predominant wind direction indicated by the wind rose.

The conditional probability plots for the total concentration of 11.5 nm particles and 65 nm particles is presented in Figure 9. These plots reveal the wind conditions at the two fixed sites north and south of the airport under high concentration situations (greater than 90th percentile of the observed values). This plot further demonstrates that the association between wind direction and total UFP count is strongly associated with the smallest diameter particles (11.5 nm). The probability of high concentrations of 65 nm particle concentration is clearly not associated with wind direction and speed. When the wind is blowing from the south, aircraft tend to land from the north (into the wind), and thus the site north of the runways experiences high concentrations of smaller 11.5 nm particles. Conversely, when the wind is blowing from the north, aircraft tend to land from the south (into the wind), and the site south of runways experiences high concentrations of the 11.5 nm particles. These relationships are consistent with those observed in Figure 9.

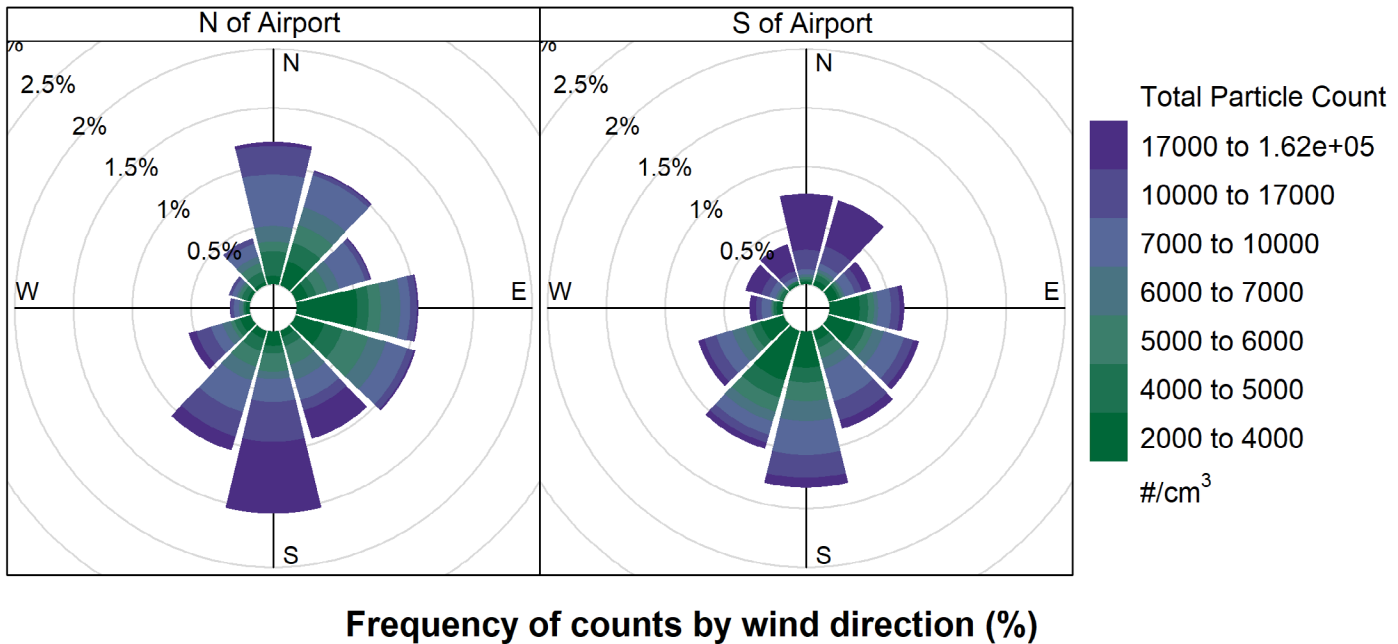
Figure 8: Wind Rose (A) and Pollutant Rose (B) at the fixed-site locations north and south of the airport.

A. Wind Rose



Frequency of counts by wind direction (%)

B. Pollution Rose



Frequency of counts by wind direction (%)

Figure 8 - To interpret (A): This wind rose plots the wind direction and wind speed observed at the two fixed sites. The spokes of the figure correspond to the percentage of times that wind is blowing from a given cardinal direction. The colors represent the wind speeds associated with a given direction. To interpret (B): The spokes of this figure represent the percentage of 15-minute wind values coming a given direction. The colors on the figure correspond to ranges of Total Particle Count associated with each wind direction. The dark purple color corresponds to the highest concentration of particles and the dark green represents the lowest concentration of particles.

Figure 9: Conditional probability plot of the pollutant concentrations at the two fixed-site locations, north and south of the airport.

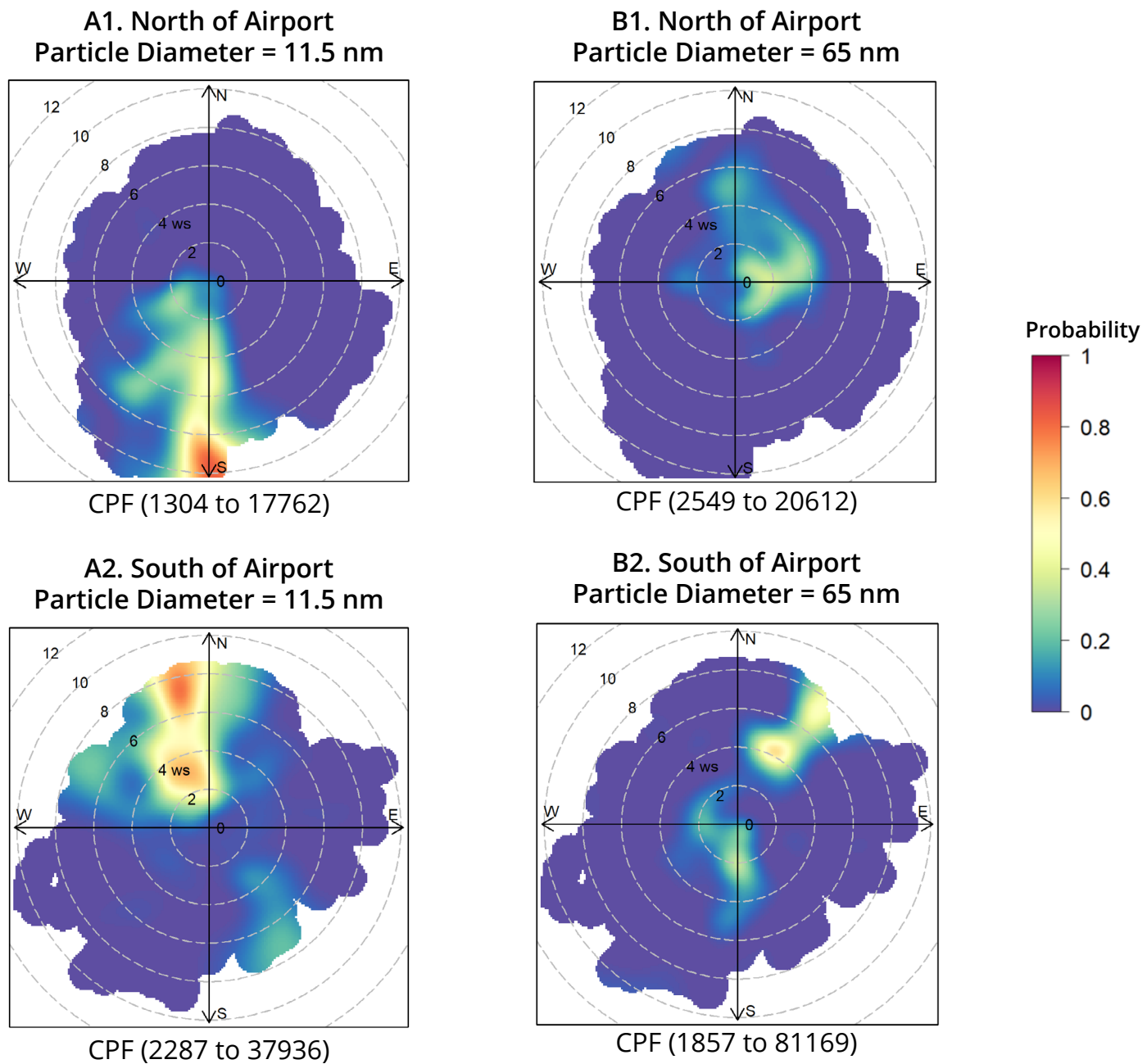


Figure 9 - These plots show the conditional probability function (CPF) that a given wind direction and wind speed occur when high concentrations of a) 11.5 nm particles (Ultra-UF) and b) 65 nm particles (UF) are measured at the North of Airport (SeaTacCC) and South of Airport (Maywood) fixed site locations.

Flight Data

To better understand the temporal pattern in flight we analyzed the 2018 data we obtained from FAA. There were 13 days of missing data (December 19-31 2018) in our data set. At Sea-Tac, there were 188,474 tracked departures. In contrast, there were a total of 27,817 tracked departures from King County International Airport (Boeing Field). On average, there are 23 arrivals per hour per day. Typically, from 6 AM until midnight there are more than 20 flights arriving per hour (Figure 10). The geographic distribution of the landing and departing flights concentrates north and south of the runways at Sea-Tac and Boeing Field. The vast majority of tracked flights are directly north and south of the western-most runway at Sea-Tac. Locations in this track typically see more than 200,000 individual aircrafts (departing and landing) at an altitude lower than 750 m in a year (Figure 11).

Figure 10: Number of flight arrivals per hour of day in 2018 at Sea-Tac Airport.

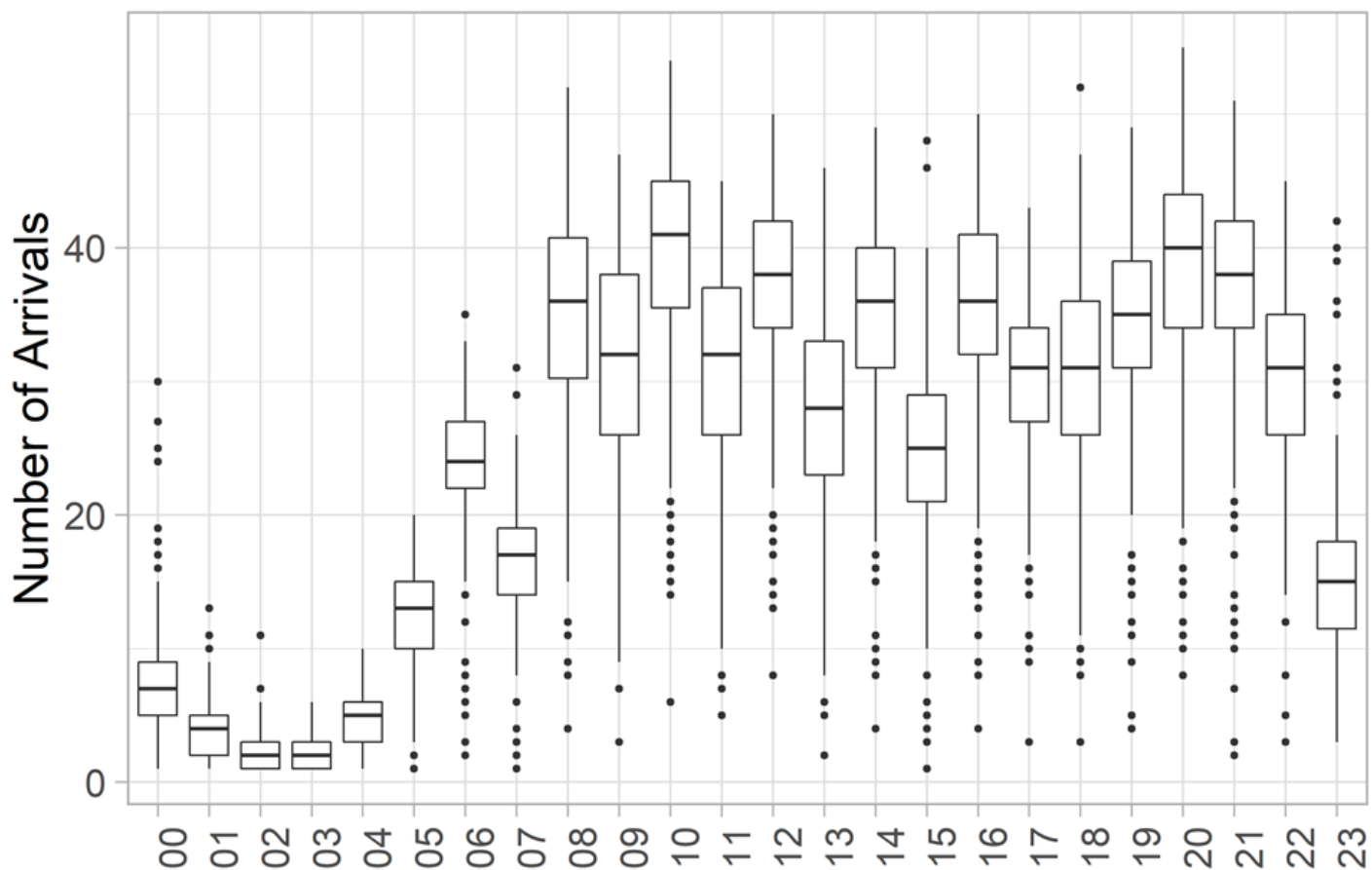


Figure 10 – The median number of arrivals is the line dividing each box; the upper and lower quartiles define the ends of the boxes. The minimum and maximum data points are drawn as points at the ends of the lines (whiskers) extending from the box.



Figure 11: The gridded spatial distribution of the number of arriving and departing flights that are below 750 m in altitude in the year 2018 for the Seattle metropolitan area.

Flights below 750m

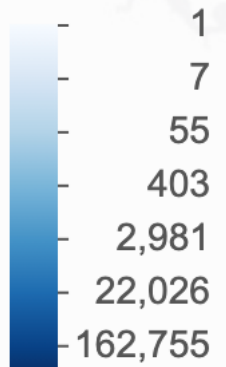


Figure 11 – The data includes flights from all local airports.

Mobile Monitoring Results

We conducted mobile monitoring with either one or two vehicles for the 63-day domain of our study between February 7th, 2018 and January 11th, 2019. Typically, the two vehicles sampled for five hours within the interval from approximately 11:00 to 17:00 on different routes – either along five transects to the north or along five transects (or six during the summer season) to the south of Sea-Tac. Overall, the airport was in south flow operation (planes taking-off to the south and landing from the north) 67% of our sampling times. This is comparable to the overall yearly proportion of south flow operation of 65% (Table 4). The wind-rose plots (Figure 12) are separated by north and south flow operating conditions derived from the flight-track data. As expected, during north flow operation, winds are predominantly from the north and northwest, whereas during south flow operation winds are from the south and southwest. There are fewer time periods with winds exceeding 6 m/s during the north flow operations, for our sampled data.

Table 4: Summary of drive days across the four seasons of the MOV-UP study

Season	Sampling days	Second car proportion	Start hour	End hour	Temp	RH	South Flow Operation
Spring	14 days	71%	11:00	16:30	65F	50%	52%
Summer	16 days	81%	11:00	17:00	73F	47%	75%
Fall	12 days	83%	11:00	17:00	54F	78%	91%
Winter	21 days	62%	11:30	17:00	51F	62%	59%

Figure 12: Wind Rose Plots. Represents the wind speed and direction over the course of all mobile monitoring sampling campaigns, separated by the landing direction of the aircraft.

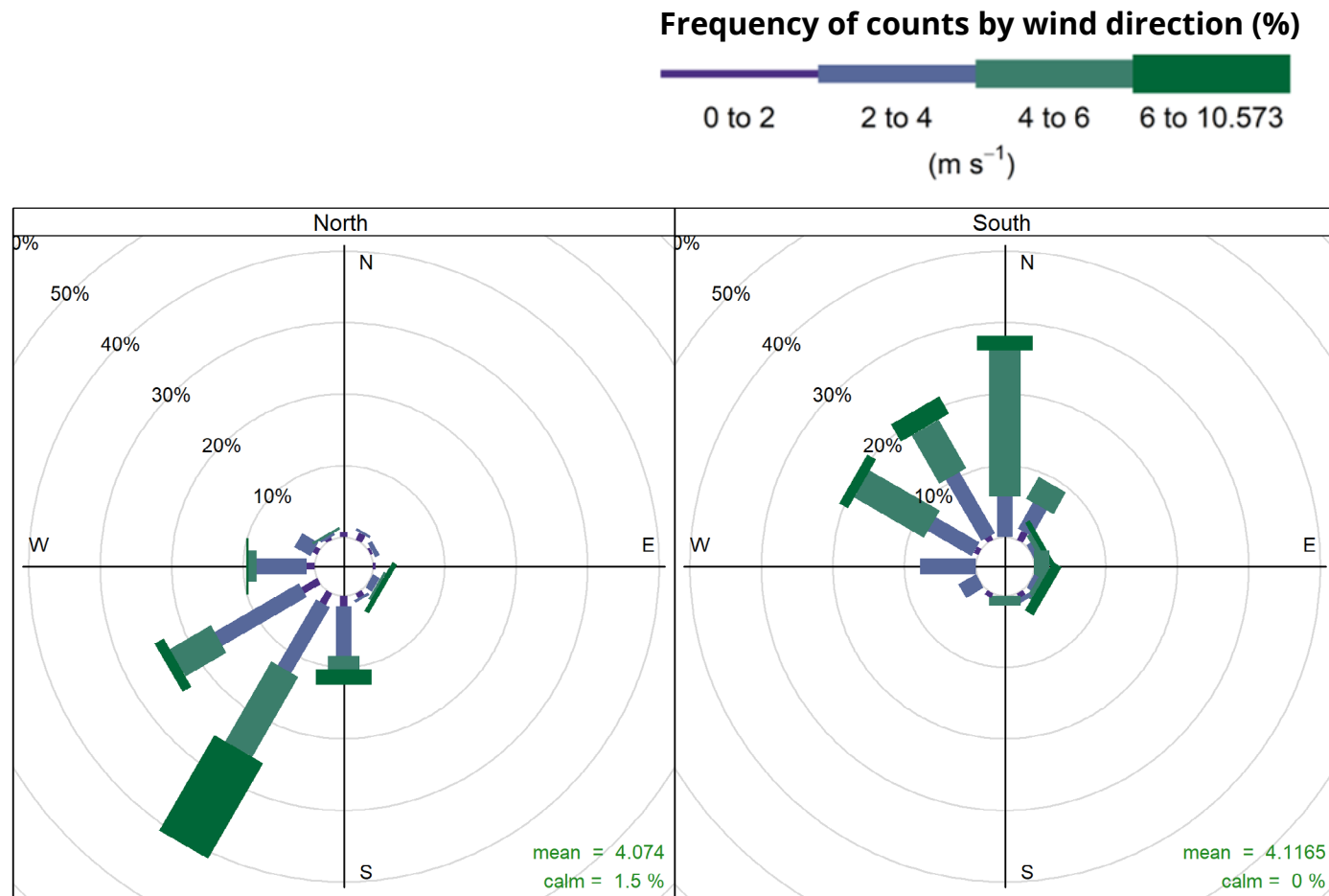


Figure 12 – The north and south labels on the plot refer to the direction from which aircraft were landing with respect to the airport.

We compared the overall concentration of roadway pollutants, on our transects, on I-5 and on SR-99 (Table 5) along with the total sampling time (in minutes) along each route segment. For the particles and gases measured, we reported the highest mean values on roads, both I-5 and SR 99. Colors in this table order the measures of each column by pollutant type. Darker purple corresponds to the highest value and white the lowest.

The mean concentration of black carbon observed on I-5 was $5.0 \mu\text{g}/\text{m}^3$ with a standard deviation of $4.3 \mu\text{g}/\text{m}^3$, whereas on transect N1 and S1, directly adjacent to the airport on north and south ends, respectively, the mean concentration of black carbon was $1.0 (\text{SD}=1.0) \mu\text{g}/\text{m}^3$ and $1.5 (\text{SD}=5.1) \mu\text{g}/\text{m}^3$ respectively. The total particle concentration measured on I-5 was $59,896(37,704) \#/cm^3$, which is significantly higher than concentrations observed along transects.

Table 5: Summary measures from the mobile monitoring campaign by monitoring location and transect.

Transect	Mean	Interquartile Range (IQR)	Standard Deviation (SD)	Minutes of Data
Aethalometer (Black Carbon: ng/m ³)				
I-5	5030	3916	4319	2155
N1	953	733	1013	3935
N2	909	618	1133	3184
N3	1280	972	1779	3073
N4	1720	1421	2504	1911
N5	1590	1320	13867	1576
S1	1544	1023	5149	1140
S2	1243	985	1264	1454
S3	1290	1068	1908	571
S4	2832	2396	13326	608
S5	1566	1984	1545	916
S6	3457	868	1008	123
SR 99	2043	1992	2089	431
Carbon Dioxide Analyzer (Carbon Dioxide : ppm)				
I-5	513	55	56	1640
N1	450	40	128	3306
N2	434	32	88	2616
N3	456	51	110	2495
N4	474	54	135	1508
N5	472	63	115	1269
S1	454	32	161	1011
S2	476	40	190	1217
S3	462	26	170	528
S4	485	38	162	559
S5	468	36	77	783
S6	443	24	19	123
SR 99	480	66	155	349
Condensation Particle Counter (Total UFP (10-1000 nm): #/cm ³)				
I-5	59896	41833	37704	2121
N1	20160	18022	16555	3853
N2	18318	15581	15260	3161
N3	20124	16747	18975	3184
N4	23186	16487	20715	1917
N5	19868	14132	19123	1606
S1	16340	12139	21452	1139
S2	19150	15202	16831	1430
S3	13433	8056	14088	567
S4	18723	13787	19496	606
S5	14500	10819	11427	903
S6	9713	5589	4402	123
SR 99	26117	19768	21077	407

There was a distinction between the distribution of black carbon and total particle number (>10 nm) we obtained from the two roadway locations and I-5 (Figure 13). Traffic-related pollutants most heavily impacted the high traffic freeway location; however, extreme values (> than the 95th percentile of the data) are common on both the transect and SR 99 sites.

Figure 13: Major roadway and transect concentrations of traffic-related pollutants: Black carbon mass; Total particle (> 10 nm) number.

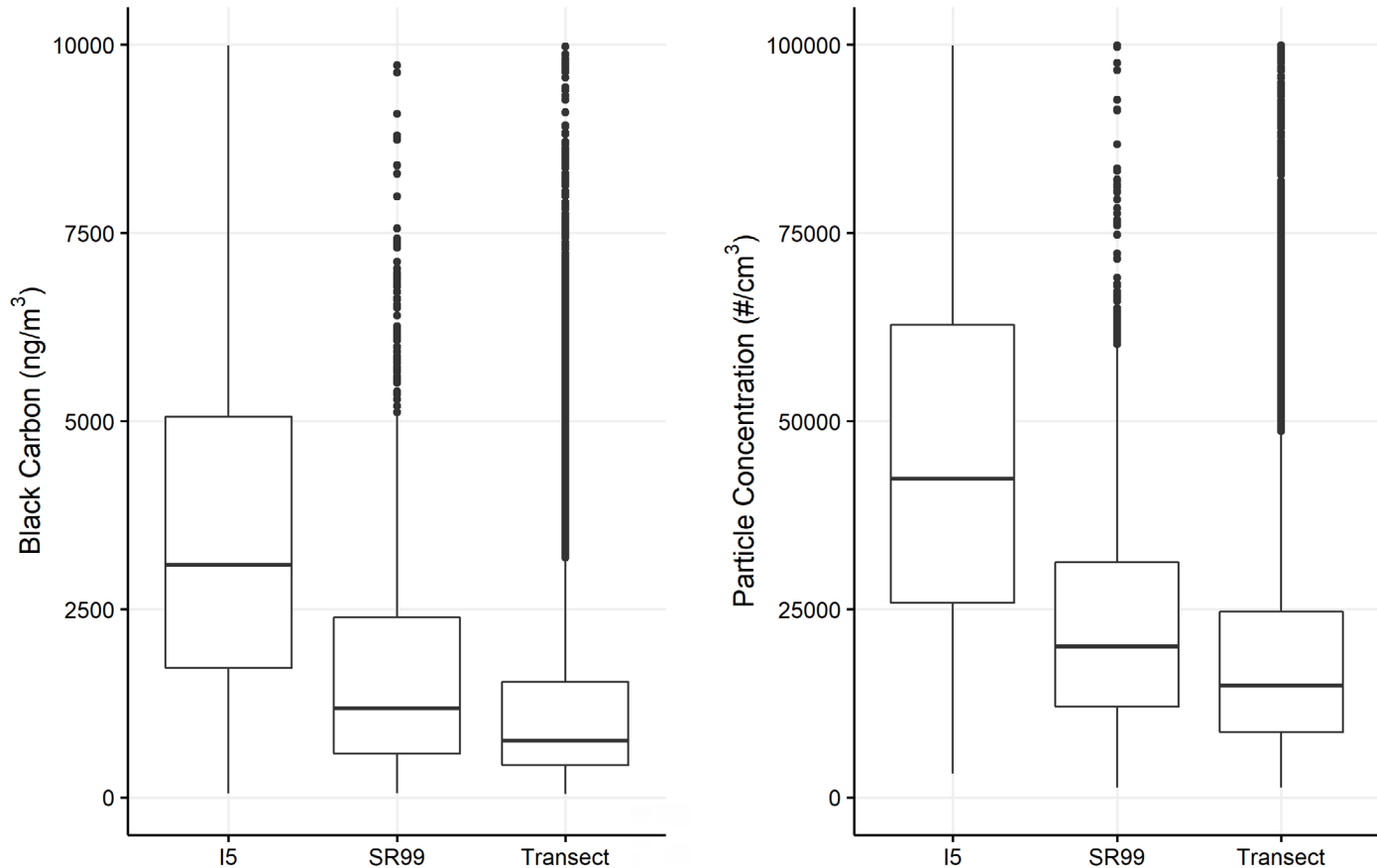
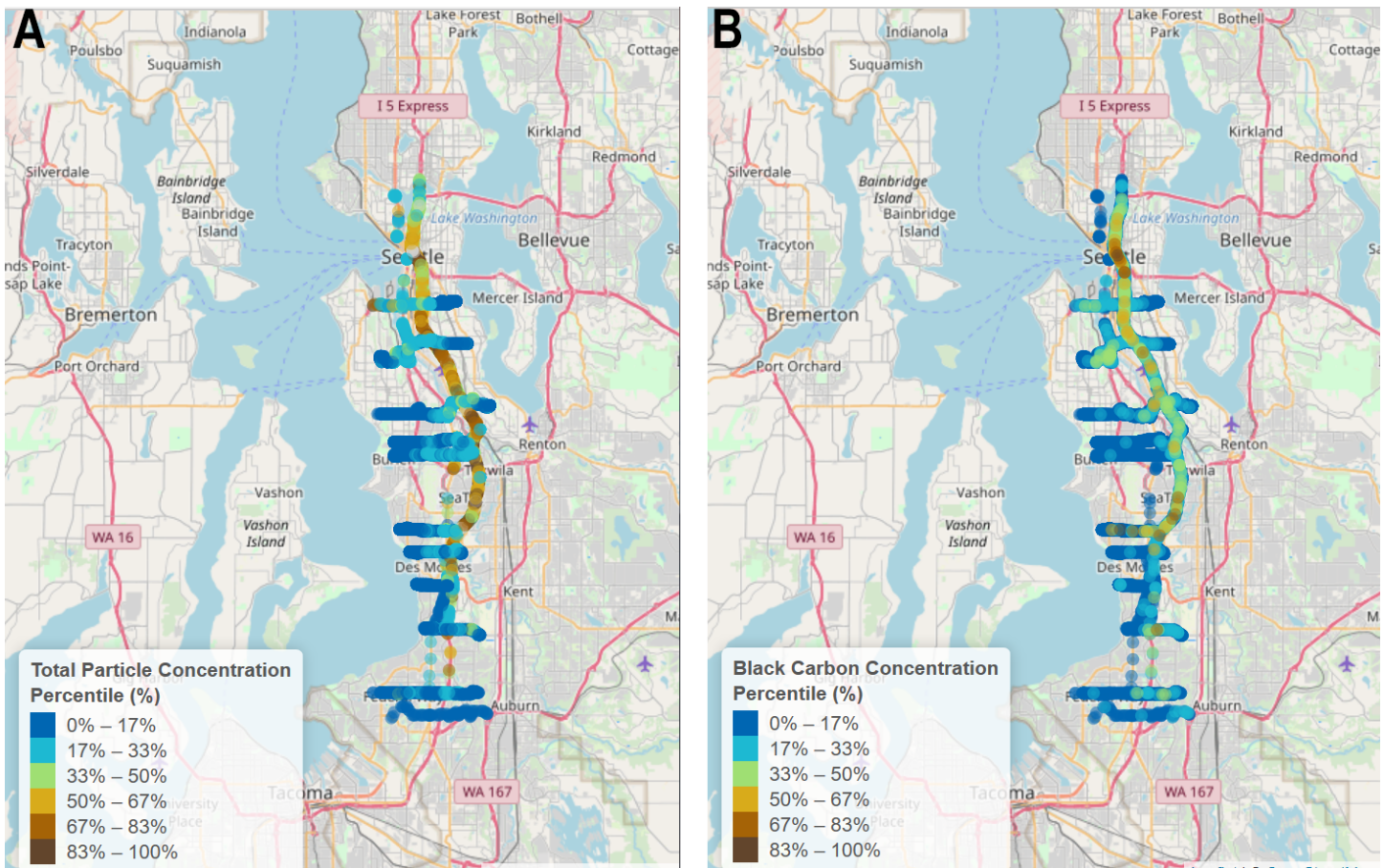


Figure 13 – This figure includes all the data collected on all transects north and south of the airport.

It is important to consider that each transect traverses along its east-west length from areas of low aircraft volume to high flight volume. Therefore, summary statistics across the entire transect may not capture peak variations. The standard deviation (SD) measures the propensity and size of the deviations in the measurements. Locations with higher standard deviations experience larger shifts in air quality over the sampling period. Typically, the highest SD values are found on road, although there are some transects that demonstrate more change in pollutant measures (high standard deviation).

The spatial distribution of traffic-related pollutants confirms that their locations are primarily on and near the major roadways. There is a clear decrease in traffic-related concentrations as the mobile monitoring platform moves away from the high-traffic locations (Figure 14).

Figure 14: Spatial distribution of traffic-related pollutant concentration percentile: A. Total particle (> 10 nm) number; B. Black carbon mass.



The PCA analysis yielded two features that together accounted for 61% of the variability in the mobile monitoring data. Figure 15 shows the factor loadings for each feature. These loadings correspond to the correlation coefficients between the pollutant variables and PCA factors. The squared factor loading is the percent of variance in that variable explained by the factor. Large positive loadings correspond to variables that have a large proportion of their variability captured within the factor. Negative loadings correspond to factors that vary inversely with the factor.

The first feature (RC1) was positively correlated with particles between 10-36 nm in diameter. In addition, this feature had negative correlation with black carbon, a pollutant primarily emitted from diesel combustion, as well as other urban sources such as rail, maritime, manufacturing and wood heating. When compared to a restricted analysis that included size-resolved information, we demonstrated a correlation of 0.82 between this feature and that which had a high association with 11.5 and 15.4 nm particles and poor association with particles greater than 20.4 nm. Based on these characteristics, we describe this as “Ultra-UF feature” for the rest of this document, as the feature is associated with landing aircraft emissions.

The second feature (RC2) from this analysis has a high correlation with particles between 20-36 nm as well as BC and Particle Number concentration. By contrast, this feature is inversely correlated with particles with a diameter smaller than 20 nm. When compared to a restricted analysis that included size resolved information, we demonstrated a correlation of 0.79 between this feature and the feature 20.4 nm. We also inversely correlated them with particles that are 11.5 nm. Based on these characteristics, we described this feature as “Roadway Feature” for the rest of this document.

Figure 15: Principal component factor loadings for each feature.

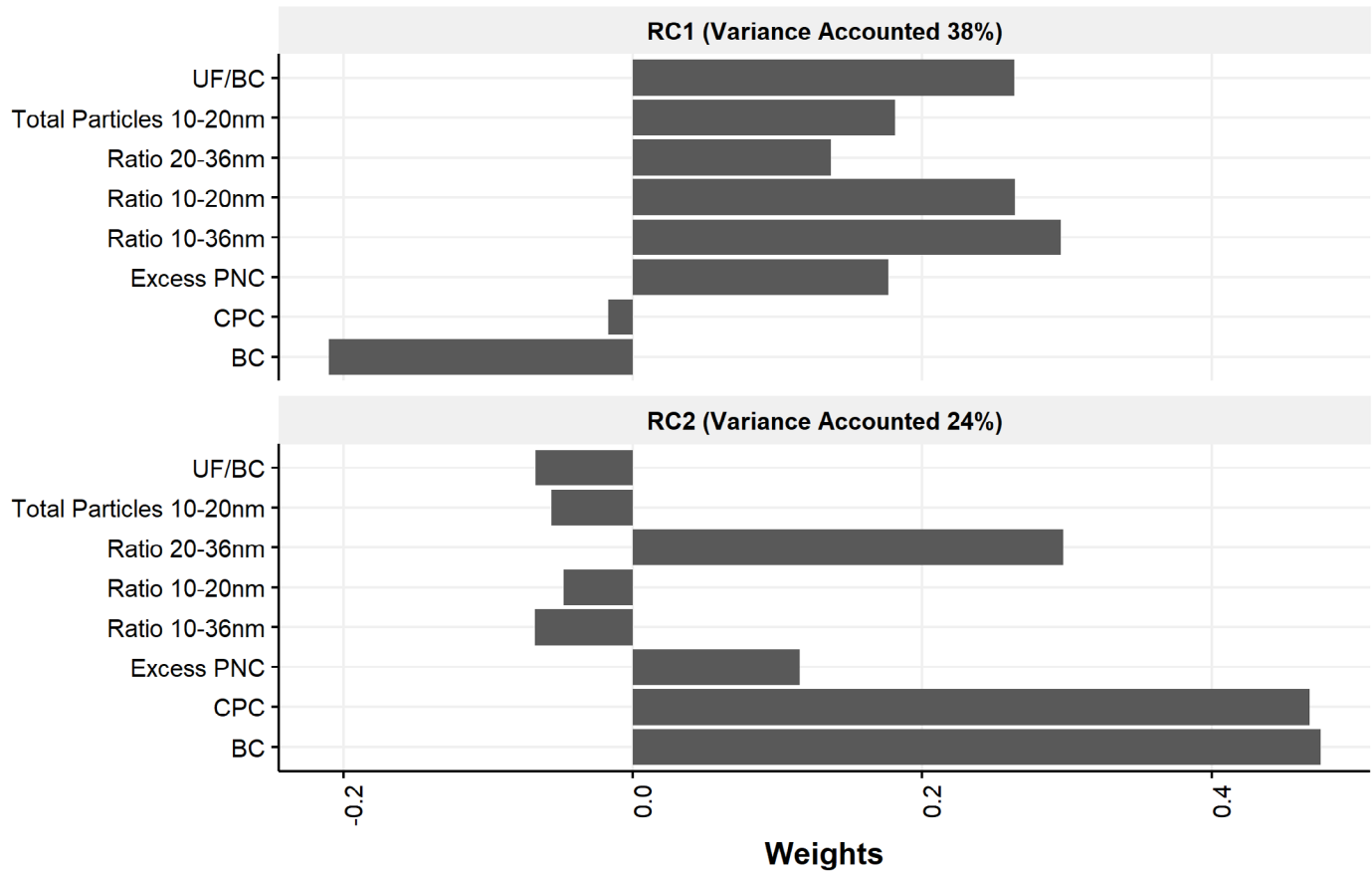


Figure 16 shows the spatial distribution of these distribution factors and plots the percentile values of the PCA scores computed over the year of sampling for each location we sampled during the mobile monitoring campaign. We can see that the roadway feature, characterized by strong correlations with roadway related pollutants, is highest overall on I-5 and at major junctions with SR-99.

Note: SR-99 runs north-south in the study domain, and the label on the map does not correspond to the East-West Transect. The Ultra-UF feature is not characterized by high concentrations on roadway. This feature shows high values north and south of the airport.

The PCA analysis demonstrated that based on the mobile monitoring campaign we can distinguish between roadway related UFP sources and a UFP source composed primarily of particles less than 20 nm in diameter. Based on previous literature,³ we believe that this fraction may be associated with aircraft emissions when aircraft engines are under light load, such as landing. To test the hypothesis that the Ultra-UF feature was associated with periods of time when aircrafts were landing overhead, we separated the data set by aircraft landing direction.

Figure 16: Spatial distribution of the “Ultra UF” PCA and the “Roadway” features.

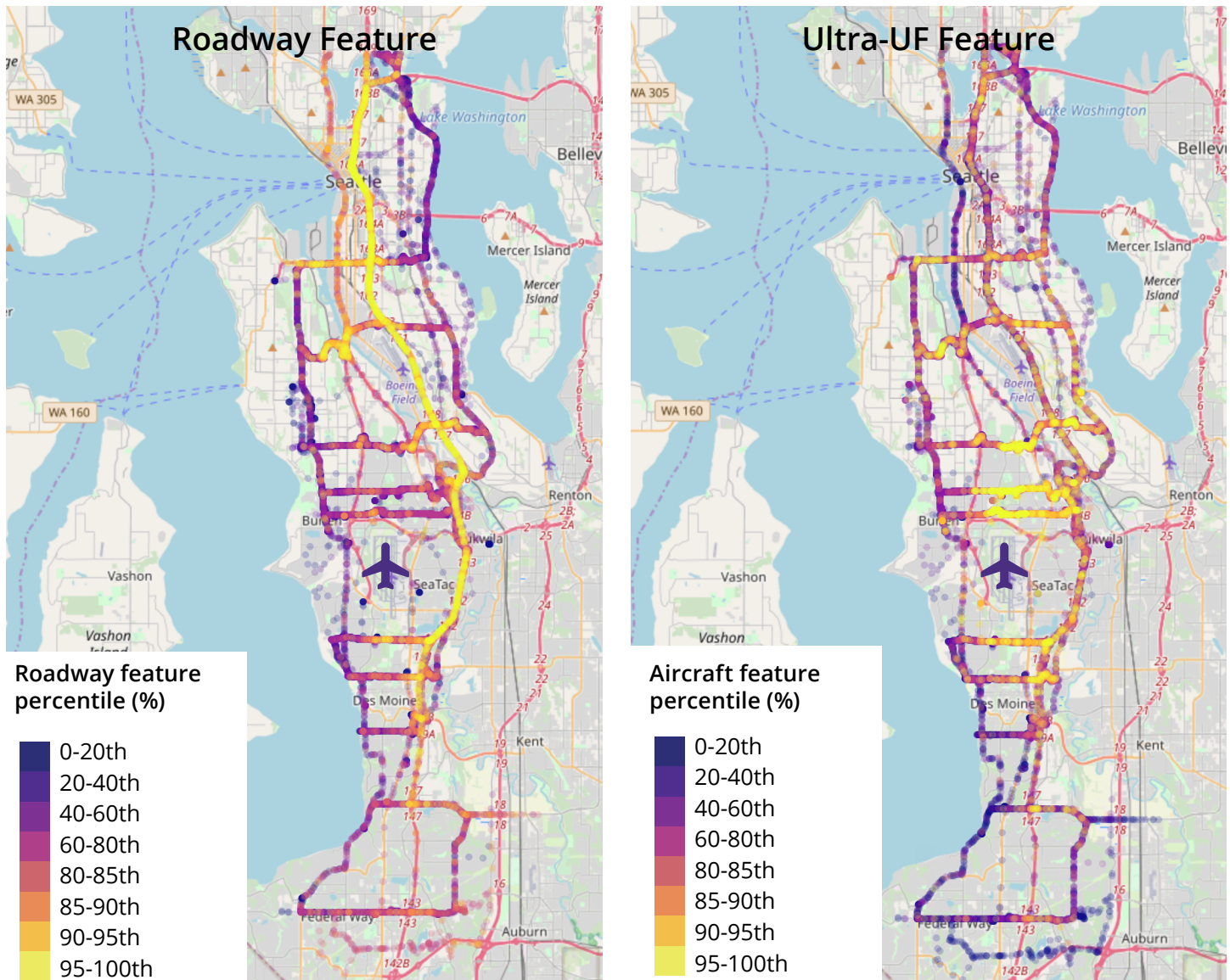


Figure 16 – Percentiles range from 0-th percentile representing the smallest observed value to 100-th representing the largest observed value. Colors correspond to percentile values for each factor score.

A high percentage of mobile monitoring measurements underneath the landing path of aircraft was consistent with the Ultra-UF feature (Figure 17). There are still some areas opposite to the landing that show some high PCA scores; these may be due to emissions from aircraft take-offs, or sometimes from poor separation between traffic and aircraft emissions by the PCA.

In contrast, plotting the scores of the roadway feature by aircraft landing direction shows (Figure 18) that there is no significant impact of landing direction on the spatial distribution of this PCA score. In addition, we can see a clear spatial gradient east and west of high-traffic roadways in this mapping. Because of the association with the aircraft landing paths, rather than roadways, the Ultra-UF is likely due to pollution from aircraft emissions.

Figure 17: Spatial distribution of the “Ultra UF” PCA feature, separated by landing direction.

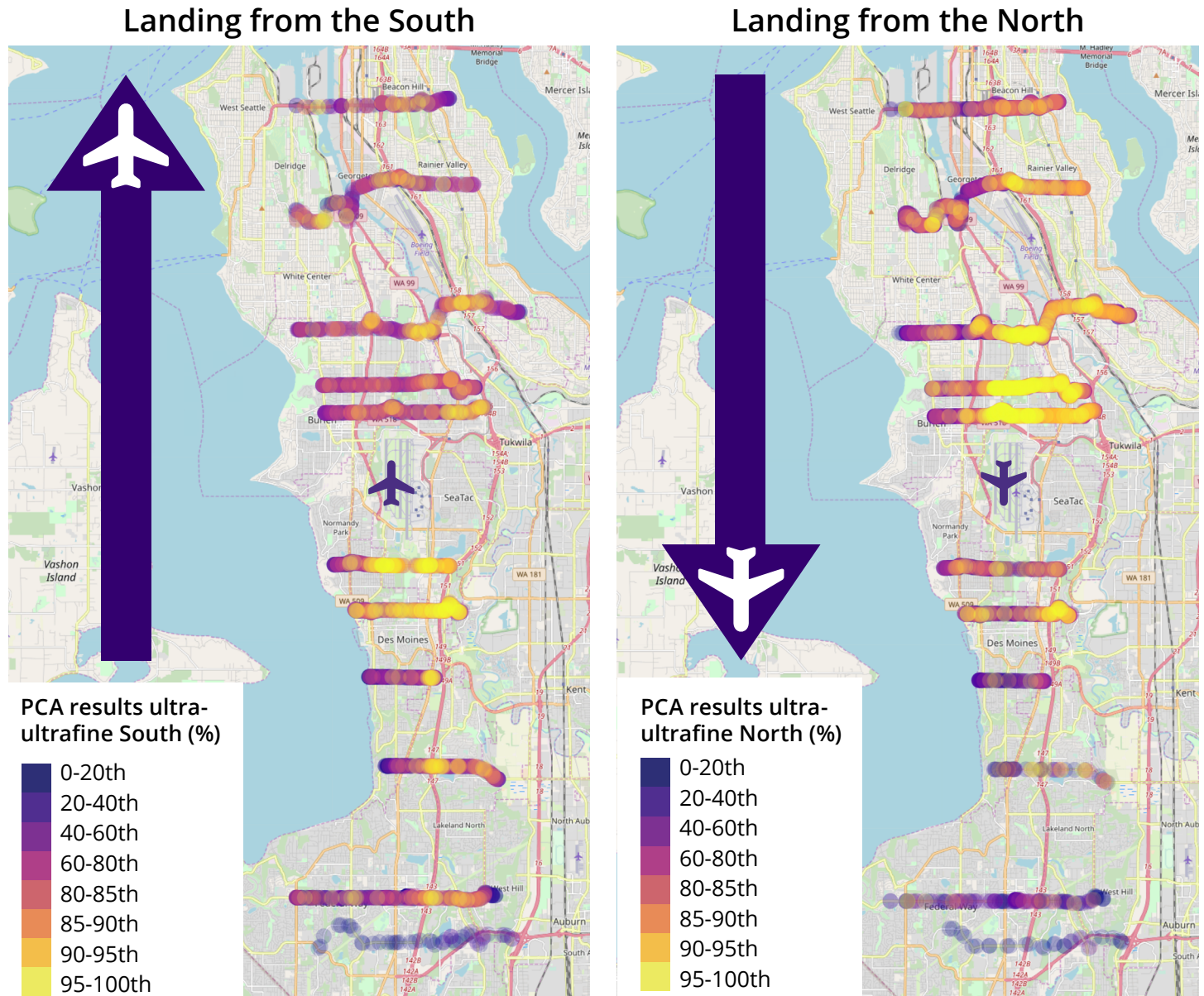


Figure 17 – Colors correspond to percentile values for the Ultra UF factor score.

Figure 18: Spatial distribution of the “Roadway” PCA feature, separated by landing direction.

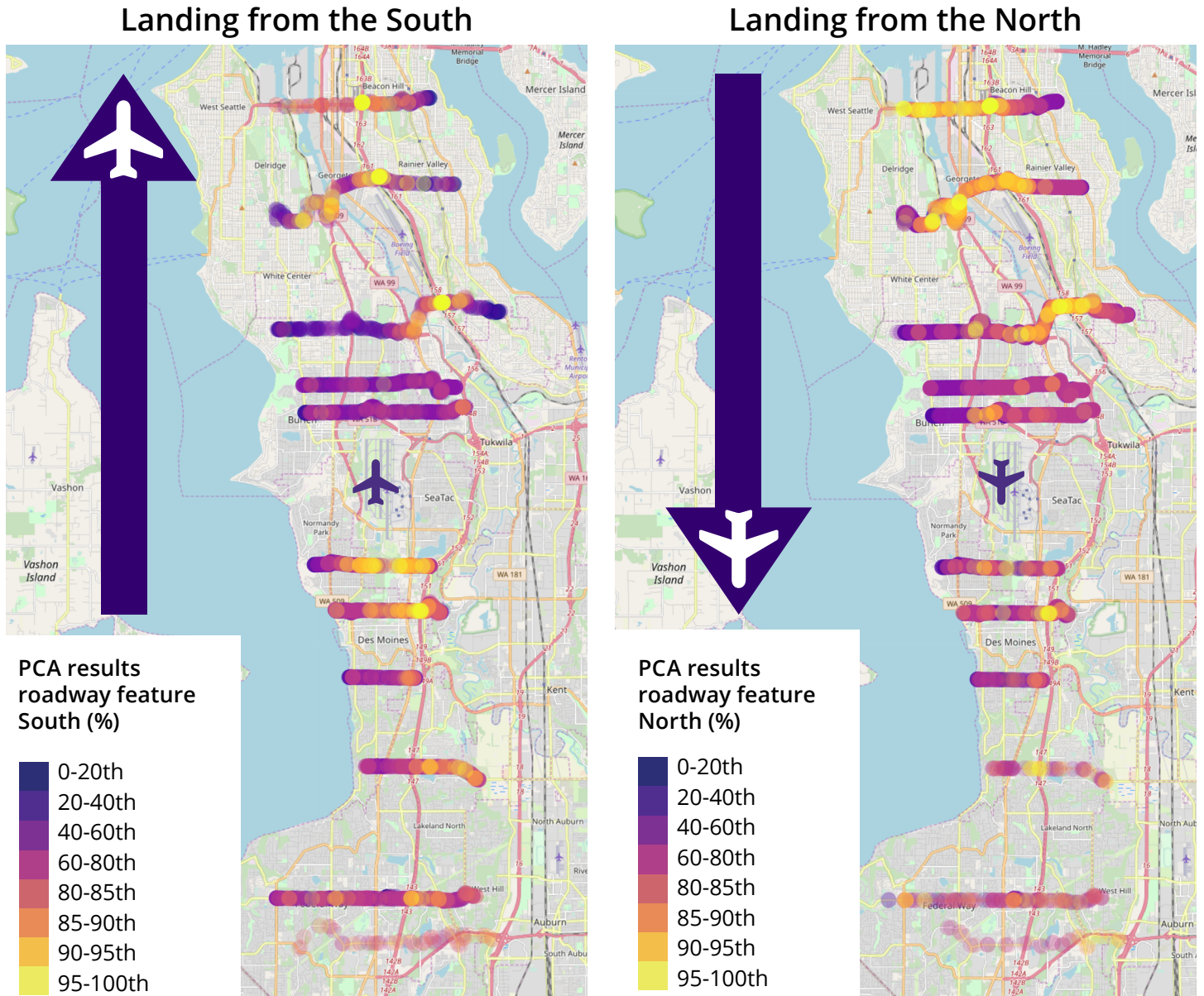


Figure 18 – Colors correspond to percentile values for the Roadway factor score.

We calculated fuel-based emission factors and grouped them by quantiles of the Roadway and Ultra UF PCA features. This emission factor represents the concentration of particles emitted per kg of fuel burned. In this study, we estimated the emission factor by the ratio of the change in particle number (10-20 nm) to the change in CO₂. The Methods section describes this calculation in detail. Over the study area, the calculated EF for the roadway feature does not significantly change (Figure 19). However, the EF at locations with high Aircraft PCA scores show a much higher emission of 10-20 nm particles than locations with a low aircraft PCA score.

Figure 19: Fuel-based emission factors calculated for quantiles of the PCA scores for the aircraft (purple) and roadway (white) features.

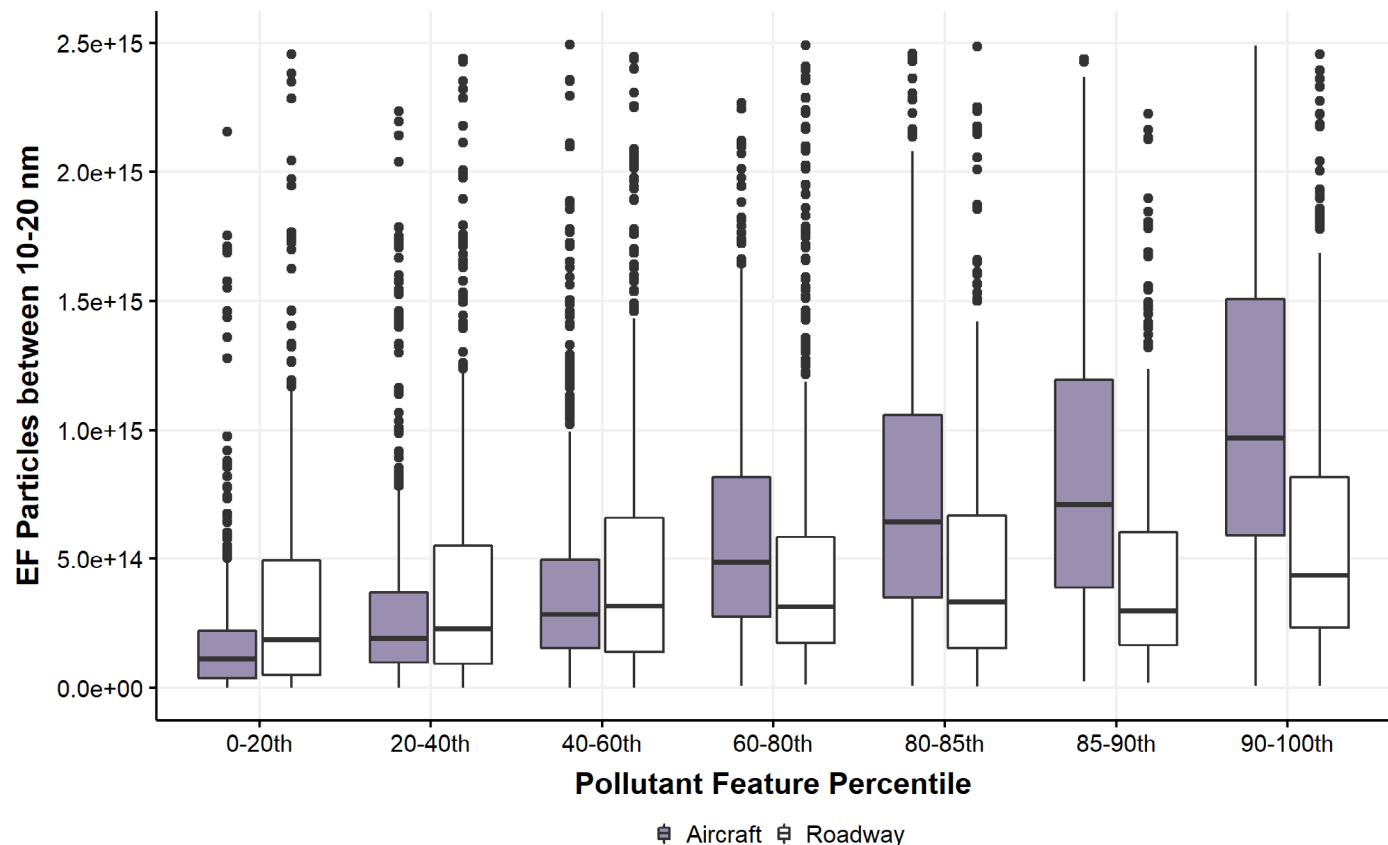


Figure 19 - Units of the EF are in #particles/Kg fuel burned.

Discussion

Main Study Findings

This is the first study of UFP concentrations near Sea-Tac Airport that distinguishes between roadway versus aircraft sources. Using a combination of fixed-site and mobile monitoring approaches conducted in four seasons throughout the year and multiple pollutant measures, we were able to distinguish aircraft-related ultrafine particles from roadway-related ultrafine particles. While ultrafine particles are emitted from both roadway traffic and aircraft, and the total concentration of UFP—particles ranging in size from 10 – 1000 nm — do not distinguish roadway traffic from aircraft, we could separate the pollution from the two sources using measurements of particle size and black carbon concentration.

Notably, comparing data collected at fixed sites near aircraft landing at Sea-Tac and a site near I-5, we observed that landing aircraft were associated with a large fraction of particles between 10-20 nm, whereas the composition of roadway traffic particles had higher black carbon content. These characteristic differences were also confirmed in analyses of the mobile monitoring data.

From a multi-pollutant PCA analysis of mobile monitoring data, we observed two features that explained the majority (61%) of the variance in the pollutant measurements. One of these features related to roadway traffic, which consisted of relatively larger ultrafine particle sizes and high black carbon concentrations. The other feature, which we termed Ultra-UF, consisted of relatively smaller ultrafine particle sizes and lower black carbon concentrations. By mapping the locations in which we measured pollution that was more likely to be either the roadway or the Ultra-UF feature, we observed that the roadway feature was located on and very near the major roadways in the study area, such as I-5 and SR-99. In contrast, we found the Ultra-UF feature below the landing paths of aircraft.

Finally, after computing fuel-based emissions factors based on the mobile monitoring data, we observed that measurements that were most consistent with the Ultra-UF feature and landing aircraft tended to have a higher emission rate of small 10-20 nm-sized particles compared to measurements that were characterized as roadway feature particles.

Our findings are consistent with previous literature on roadway and aircraft-related ultrafine particle pollution. Monitoring campaigns conducted in airport communities near Los Angeles,³ Atlanta,³⁷ Boston,^{5, 6} New York,³⁹ and Amsterdam⁷ have all identified elevated levels of UFP that aircraft have caused. The Los Angeles studies in particular found elevated concentrations of UFP underneath the aircraft landing paths of the LAX airport, and that concentrations of UFP at ground level near the airport runway tend to consist of smaller 10 – 20 nm size fractions.³

Moreover, our estimates of the emissions factor of particles from the aircraft-related Ultra-UF feature are consistent with previous studies that range in magnitude from 10^{14} to 10^{17} particles/kg fuel.⁴⁵ Also consistent with previous literature, we estimate a larger UFP impact related to aircraft landings as compared to aircraft take-offs. This is consistent with previous studies directly testing the emission factors from jet engines at different load conditions and reporting much higher emissions at 30% load.³⁸

The spatial patterns we observed for the roadway feature ultrafine particles is also consistent with previous studies. Most studies have observed elevated concentrations immediately adjacent to and downwind of major freeways.⁴⁶ From these previous studies, UFP

concentrations have been found to follow a “rapid decay” spatial pattern with a decrease in concentration by at least 50% over a distance of 150 m away from the major roadway, with gradual decay to background thereafter over a distance of 500 m. We observed similar spatial patterns for the roadway PCA feature, which was most associated with measurements on and immediately next to the major roadways in our study area, I-5 and SR-99.

In contrast, we found the spatial pattern of the aircraft-related Ultra-UF feature away from major roadways, except for a region south of Sea-Tac where the flight path is nearly above the I-5 freeway. To get a better picture of the potential extent of population exposures to aircraft-related ultrafines, and to model the potential extent of elevated ultrafine particles, we assigned emissions to aircraft landing and wind patterns observed during our study (Figure 20).

There is a relatively rapid downward transport of these aircraft-emitted UFPs and relatively little time for their physical aging due to coagulation with larger particles. This downward transport is due to a combination of large-scale daytime, convective velocities of up to one meter per second and local scale wingtip vortices that can extend vertically downward for several hundred meters at similar, superimposed velocities.⁴⁷ This results in plumes from descending aircraft reaching ground level in approximately a few minutes near the airport and up to 15 to 20 minutes at 15 km downwind from the airport.

At these plume transport times, 10 to 20 nm UFPs emitted by jet engines have a characteristic coagulation half-life of about an hour, assuming that they are emitted into a background aerosol with a number concentration of 1×10^4 particles per cubic centimeter and count mean diameter of 0.2 μm .⁴⁸ It is not surprising that the typical size of these UFPs in the downwind footprint are typically between 10 and 30 nm, indicating minimal coagulation losses.

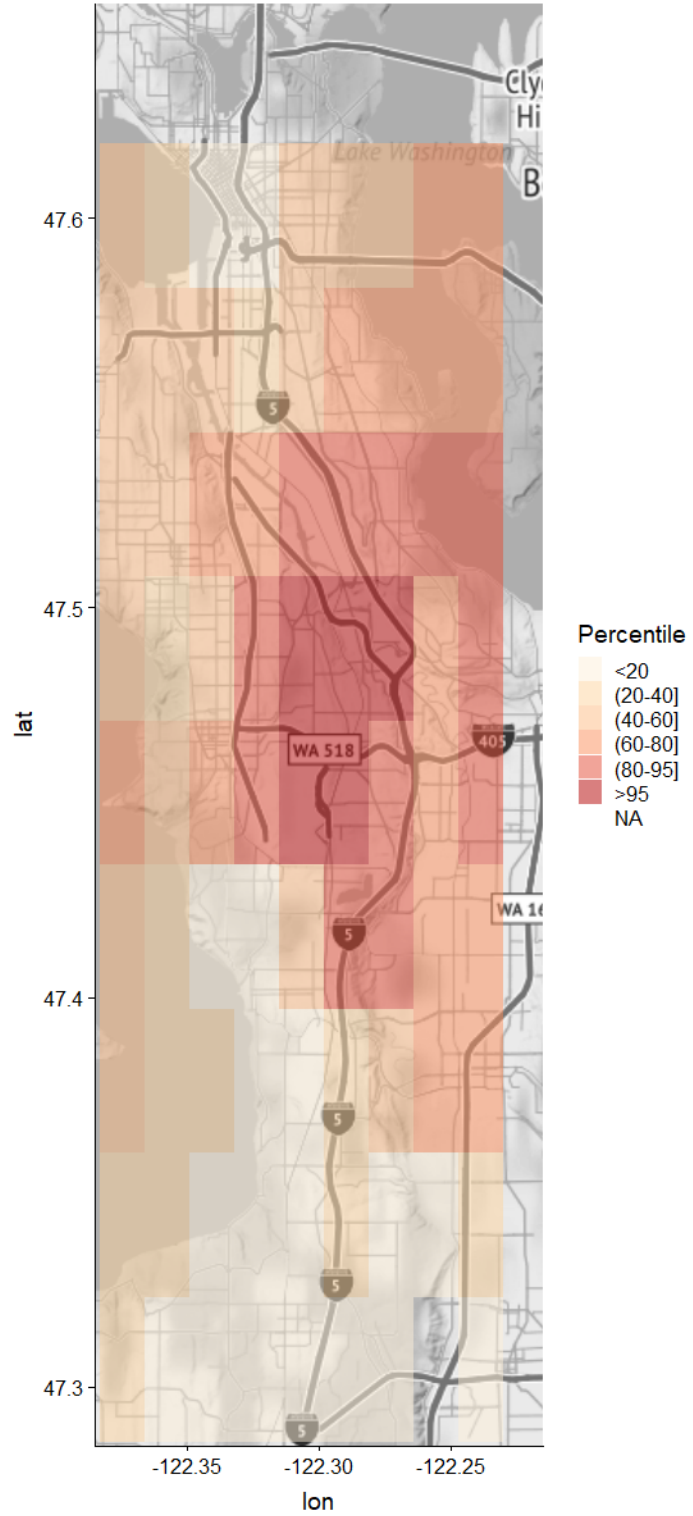
The model results are similar to the spatial pattern of the Ultra-UF PCA feature derived from mobile monitoring measurements. The air quality model results and the map of Ultra-UF from mobile monitoring both suggest that communities underneath and downwind of landing aircraft may be exposed to this source of air pollution.

The differences in the spatial extent of aircraft versus roadway traffic UFP are important to consider from a population impact perspective. We observed concentrations of total UFP (10 – 1000 nm sized particles) to be higher at the near-roadway fixed site compared to concentrations observed at the near-airport fixed sites. However, most people spend a relatively small proportion of their time on a major roadway (e.g., during commuting), and because of the relatively short distances over which roadway UFP decays downwind of major roadways, roadway UFP would affect only a narrow swath of near-roadway residences and other buildings.

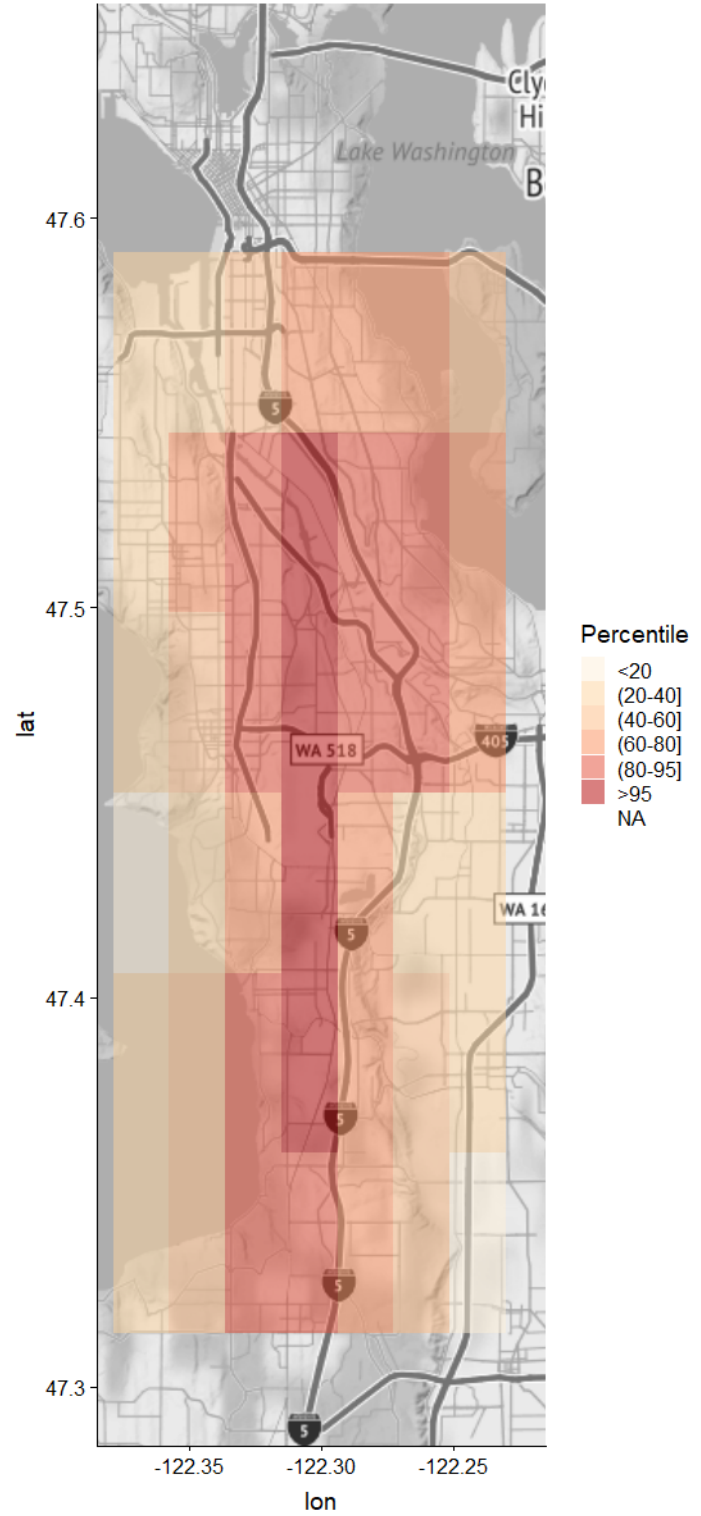
In contrast, the affected areas experiencing elevated aircraft UFP tend to be larger. Therefore, considering the map shown in Figure 20, there is the potential for more people to be affected by UFP from aircraft than from roadway sources, albeit at lower concentrations. Moreover, those living within the area affected by landing aircraft emissions may be exposed to relatively higher concentrations of smaller sized ultra-UF particles.

Figure 20: Spatial distribution of A) Ultra-UF feature from our mobile sampling and B) Aermod air quality model for UFP emissions from landing aircraft for the meteorological conditions observed during the study.

A. Mobile monitoring data



B. Aermod model predictions



Uncertainties

Some of the findings of this study are subject to limitations and uncertainties inherent to scientific study, as in the following cases:

- Although both PCA analysis and the ratio of small (e.g., 10-20 nm) to total UFP indicate a spatial pattern with aircraft activity, there is no chemical or compositional indicator that these particles are directly related to aircraft activity. Chemical composition may be possible to ascertain in future studies as described below in “Knowledge Gaps.”
- We did not observe any PCA features associated with other important urban sources of UFP, including residential wood-smoke burning, industrial emissions and atmospheric transformation of gaseous pollutants. The PCA methodology does not *a priori* exclude any pollutant features.
- We carefully maintained and calibrated our instruments as this report describes; however, the comparison between simultaneous mobile sampling in two cars or fixed-site monitoring at two locations is subject to variances between instruments.
- Inherently, time is a confounder in a mobile monitoring campaign as urban background concentrations can change significantly over time, even over the course of one mobile monitoring route. This is why we took many repeated measurements during data collection to account for some of these potential confounders. Additionally, this was the rationale in monitoring afternoon hours to minimize the effect of daily variations in atmospheric mixing height, which would influence the sampling results. Time confounding limits our ability to make comparisons between seasons of sampling given that there are approximately two weeks of sampling in each season.
- Because our fixed-site monitoring and mobile monitoring routes did not measure every possible location where people live, work and play, there is uncertainty in how our findings generalize to exposures to the population within the study area. Using the derived emissions factor and air quality modeling to estimate exposure to either roadway or aircraft-related pollution is subject to model uncertainties. This may explain some key differences between our mobile monitoring footprint and AERMOD predictions, particularly south of the airport.
- There may be impacts from other local airports that this report does not investigate.
- The scope of the current study did not consider how either roadway or aircraft traffic may be changing over time, and how these changes might affect exposures in the study area. Future studies may consider this, as “Knowledge Gaps” describes below.
- The scope of the current study did not consider how exposures to roadway or aircraft-related pollution may be related to health effects in the study area. There are already a number of studies that have considered ultrafine exposures generally and their associations with a variety of health effects, as noted in the introduction. However, there are relatively few studies that have considered aircraft-specific air pollution exposures, which is an important knowledge gap that future studies may address.

Knowledge Gaps

We identified several knowledge gaps in the process of analyzing results from this study. Many of these are outside of the scope of the initial research project but are emerging through discussion of results as well as from community input and stakeholder partnerships. With each of these knowledge gaps, there are opportunities for continued engagement with stakeholders and community scientists to generate practical, actionable information. Below are three knowledge gaps, prioritized by the Study Advisory Board.

Gap # 1: What are the health effects of aircraft UFP?

Although many studies have identified health effects associated with roadway traffic UFP, the potential health effects from aircraft-related UFP exposure still need major research. Our study highlights the need to fill this knowledge gap because we observed that particle size distribution of traffic UFP is different from aircraft UFP.

Possible Next Steps for Future Work:

- What are the chemical differences between UFP from roadway traffic and aircraft sources? The particles must be collected using an instrument capable of separating the smallest size fraction of particles from other ambient particles. We have identified instruments that are potentially useful for separating and collecting these small particles appropriate for a study that examines the chemical toxicity of these different UFP sources.
- Are short-term health responses to roadway traffic and aircraft particles different? Many studies establish short-term inflammation responses to traffic-related particles. One study demonstrates a short-term inflammation response to aircraft particles in an urban setting.³¹ We could conduct a study of short-term health impacts on sensitive populations, such as pregnant women, children, older adults or individuals with pre-existing disease (asthmatics, diabetics and those with poor cardiovascular health).
- Are there long-term health impacts of exposure to traffic and aircraft UFP? Developing an appropriate cohort, health outcome and time-scale is possible, but requires consultation with the Washington State Department of Health and community members to identify the most feasible and important populations and health outcomes to consider. Some study advisory members emphasize the difficulty of conducting a large long-term cohort study and the need to account for potential confounders.

Gap # 2: What can we do to reduce human exposures to UFP?

Our study suggests that the population in some neighborhoods may have more exposure to UFP than others due to proximity to roadway traffic and/or overlap with the plumes from aircraft emissions. It is unclear what the most effective short- and long-term approaches are to reduce human exposures to UFP.

Possible Next Steps for Future Work:

- How much of UFP infiltrates into indoor spaces, particularly schools, daycares, elder care facilities and medical centers where UFP could potentially expose vulnerable populations? What interventions are effective in reducing exposures to UFP in these community settings? We could design a study that considers, for example, the effectiveness of HEPA filtration, whether noise mitigations might alter infiltration or whether LEED buildings or HVAC choices could alter infiltration.

- What are the potential impacts of emissions reductions on exposure? We could design a study that models how changes in emissions might impact exposures to different populations.

Gap # 3: How are exposures to UFP changing over time in different communities?

Our study suggests that some neighborhoods may be more exposed to UFP than others due to proximity to roadway traffic and/or overlap with the plumes from aircraft emissions. Roadway and aircraft traffic have changed in volume, travel patterns and per-unit emissions over time, and will likely continue to change, creating uncertainties in the impacts of future UFP exposures.

Possible Next Steps for Future Work:

- Are there important daily and seasonal and time trends in exposures? We could design a study that systematically monitors and models the impacts of changing roadway and aircraft traffic on UFP exposures. This work would potentially allow us to predict UFP concentrations at locations and time-periods where no one has collected exposure data.

Bibliography

1. Seattle, Port of, Airport Statistics. <https://www.portseattle.org/page/airport-statistics>. (Ocotober 8, 2019),
2. Ross, M. A., Integrated science assessment for particulate matter. US Environmental Protection Agency: Washington DC, USA **2009**, 61-161.
3. Hudda, N.; Fruin, S., International airport impacts to air quality: size and related properties of large increases in ultrafine particle number concentrations. *Environ. Sci. Technol.* **2016**, 50 (7), 3362-3370.
4. Hudda, N.; Gould, T.; Hartin, K.; Larson, T. V.; Fruin, S. A., Emissions from an international airport increase particle number concentrations 4-fold at 10 km downwind. *Environ. Sci. Technol.* **2014**, 48 (12), 6628-6635.
5. Hudda, N.; Simon, M.; Zamore, W.; Durant, J., Aviation-Related impacts on ultrafine particle number concentrations outside and inside residences near an airport. *Environ. Sci. Technol.* **2018**, 52 (4), 1765-1772.
6. Hudda, N.; Simon, M.; Zamore, W.; Brugge, D.; Durant, J., Aviation emissions impact ambient ultrafine particle concentrations in the greater Boston area. *Environ. Sci. Technol.* **2016**, 50 (16), 8514-8521.
7. Keuken, M.; Moerman, M.; Zandveld, P.; Henzing, J.; Hoek, G., Total and size-resolved particle number and black carbon concentrations in urban areas near Schiphol airport (the Netherlands). *Atmos. Environ.* **2015**, 104, 132-142.
8. Sabaliauskas, K.; Jeong, C.-H.; Yao, X.; Reali, C.; Sun, T.; Evans, G. J., Development of a land-use regression model for ultrafine particles in Toronto, Canada. *Atmos. Environ.* **2015**, 110, 84-92.
9. Shairsingh, K. K.; Jeong, C.-H.; Wang, J. M.; Evans, G. J., Characterizing the spatial variability of local and background concentration signals for air pollution at the neighbourhood scale. *Atmos. Environ.* **2018**, 183, 57-68.
10. Weichenthal, S.; Van Ryswyk, K.; Goldstein, A.; Shekarrizfard, M.; Hatzopoulou, M., Characterizing the spatial distribution of ambient ultrafine particles in Toronto, Canada: A land use regression model. *Environ. Pollut.* **2016**, 208, 241-248.
11. Levy, I.; Mihele, C.; Lu, G.; Narayan, J.; Hilker, N.; Brook, J., Elucidating multipollutant exposure across a complex metropolitan area by systematic deployment of a mobile laboratory. *Atmospheric Chemistry and Physics* **2014**, 14 (14), 7173-7193.
12. Baldwin, N.; Gilani, O.; Raja, S.; Batterman, S.; Ganguly, R.; Hopke, P.; Berrocal, V.; Robins, T.; Hoogterp, S., Factors affecting pollutant concentrations in the near-road environment. *Atmos. Environ.* **2015**, 115, 223-235.
13. Patton, A. P.; Perkins, J.; Zamore, W.; Levy, J. I.; Brugge, D.; Durant, J. L., Spatial and temporal differences in traffic-related air pollution in three urban neighborhoods near an interstate highway. *Atmos. Environ.* **2014**, 99, 309-321.
14. Hu, S.; Paulson, S. E.; Fruin, S.; Kozawa, K.; Mara, S.; Winer, A. M., Observation of elevated air pollutant concentrations in a residential neighborhood of Los Angeles California using a mobile platform. *Atmos. Environ.* **2012**, 51, 311-319.

15. Hagler, G. S.; Thoma, E. D.; Baldauf, R. W., High-resolution mobile monitoring of carbon monoxide and ultrafine particle concentrations in a near-road environment. *J. Air Waste Manage. Assoc.* **2010**, 60 (3), 328-336.
16. Westerdahl, D.; Fruin, S.; Sax, T.; Fine, P. M.; Sioutas, C., Mobile platform measurements of ultrafine particles and associated pollutant concentrations on freeways and residential streets in Los Angeles. *Atmos. Environ.* **2005**, 39 (20), 3597-3610.
17. Pekkanen, J.; Kulmala, M., Exposure assessment of ultrafine particles in epidemiologic time-series studies. *Scand. J. Work Environ. Health* **2004**, 30, 9-18.
18. Hoek, G.; Boogaard, H.; Knol, A.; De Hartog, J.; Slottje, P.; Ayres, J. G.; Borm, P.; Brunekreef, B.; Donaldson, K.; Forastiere, F., Concentration response functions for ultrafine particles and all-cause mortality and hospital admissions: results of a European expert panel elicitation. *Environ. Sci. Technol.* **2009**, 44 (1), 476-482.
19. Seaton, A.; Godden, D.; MacNee, W.; Donaldson, K., Particulate air pollution and acute health effects. *The lancet* **1995**, 345 (8943), 176-178.
20. Natusch, D. F.; Wallace, J. R., Urban aerosol toxicity: the influence of particle size. *Science* **1974**, 186 (4165), 695-699.
21. Goldberg, M. S.; Labrèche, F.; Weichenthal, S.; Lavigne, E.; Valois, M.-F.; Hatzopoulou, M.; Van Ryswyk, K.; Shekarrizfard, M.; Villeneuve, P. J.; Crouse, D., The association between the incidence of postmenopausal breast cancer and concentrations at street-level of nitrogen dioxide and ultrafine particles. *Environ. Res.* **2017**, 158, 7-15.
22. Ostro, B.; Hu, J.; Goldberg, D.; Reynolds, P.; Hertz, A.; Bernstein, L.; Kleeman, M. J., Associations of mortality with long-term exposures to fine and ultrafine particles, species and sources: results from the California Teachers Study Cohort. *Environ. Health Perspect.* **2015**, 123 (6), 549-556.
23. Corlin, L.; Ball, S.; Woodin, M.; Patton, A.; Lane, K.; Durant, J.; Brugge, D., Relationship of Time-Activity-Adjusted Particle Number Concentration with Blood Pressure. *Int. J. Env. Res. Public Health* **2018**, 15 (9), 2036.
24. Bai, L.; Weichenthal, S.; Kwong, J. C.; Burnett, R. T.; Hatzopoulou, M.; Jerrett, M.; van Donkelaar, A.; Martin, R. V.; Van Ryswyk, K.; Lu, H., Associations of Long-Term Exposure to Ultrafine Particles and Nitrogen Dioxide With Increased Incidence of Congestive Heart Failure and Acute Myocardial Infarction. *Am. J. Epidemiol.* **2018**, 188 (1), 151-159.
25. Rich, D. Q.; Peters, A.; Schneider, A.; Zareba, W.; Breitner, S.; Oakes, D.; Wiltshire, J.; Kane, C.; Frampton, M. W.; Hampel, R., Ambient and Controlled Particle Exposures as Triggers for Acute ECG Changes. Research report (Health Effects Institute) **2016**, (186), 5-75.
26. Weichenthal, S.; Hatzopoulou, M.; Goldberg, M. S., Exposure to traffic-related air pollution during physical activity and acute changes in blood pressure, autonomic and micro-vascular function in women: a cross-over study. Part. Fibre Toxicol. **2014**, 11 (1), 70.
27. Weichenthal, S.; Lavigne, E.; Valois, M.-F.; Hatzopoulou, M.; Van Ryswyk, K.; Shekarrizfard, M.; Villeneuve, P. J.; Goldberg, M. S.; Parent, M.-E., Spatial variations in ambient ultrafine particle concentrations and the risk of incident prostate cancer: A case-control study. *Environ. Res.* **2017**, 156, 374-380.
28. Weichenthal, S.; Bai, L.; Hatzopoulou, M.; Van Ryswyk, K.; Kwong, J. C.; Jerrett, M.; van Donkelaar, A.; Martin, R. V.; Burnett, R. T.; Lu, H., Long-term exposure to ambient ultrafine

particles and respiratory disease incidence in Toronto, Canada: a cohort study. *Environ. Health* **2017**, *16* (1), 64.

29. Cass, G. R.; Hughes, L. A.; Bhave, P.; Kleeman, M. J.; Allen, J. O.; Salmon, L. G., The chemical composition of atmospheric ultrafine particles. *Philosophical Transactions of the Royal Society of London. Series A: Mathematical, Physical and Engineering Sciences* **2000**, *358* (1775), 2581-2592.

30. Zhu, Y.; Hinds, W. C.; Kim, S.; Shen, S.; Sioutas, C., Study of ultrafine particles near a major highway with heavy-duty diesel traffic. *Atmos. Environ.* **2002**, *36* (27), 4323-4335.

31. Hagler, G.; Baldauf, R.; Thoma, E.; Long, T.; Snow, R.; Kinsey, J.; Oudejans, L.; Gullett, B., Ultrafine particles near a major roadway in Raleigh, North Carolina: Downwind attenuation and correlation with traffic-related pollutants. *Atmos. Environ.* **2009**, *43* (6), 1229-1234.

32. Riley, E. A.; Banks, L.; Fintzi, J.; Gould, T. R.; Hartin, K.; Schaal, L.; Davey, M.; Sheppard, L.; Larson, T.; Yost, M. G., Multi-pollutant mobile platform measurements of air pollutants adjacent to a major roadway. *Atmos. Environ.* **2014**, *98*, 492-499.

33. Holmén, B. A.; Ayala, A., Ultrafine PM emissions from natural gas, oxidation-catalyst diesel, and particle-trap diesel heavy-duty transit buses. *Environ. Sci. Technol.* **2002**, *36* (23), 5041-5050.

34. Fruin, S.; Westerdahl, D.; Sax, T.; Sioutas, C.; Fine, P., Measurements and predictors of on-road ultrafine particle concentrations and associated pollutants in Los Angeles. *Atmos. Environ.* **2008**, *42* (2), 207-219.

35. Westerdahl, D.; Wang, X.; Pan, X.; Zhang, K. M., Characterization of on-road vehicle emission factors and microenvironmental air quality in Beijing, China. *Atmos. Environ.* **2009**, *43* (3), 697-705.

36. Larson, T.; Gould, T.; Riley, E. A.; Austin, E.; Fintzi, J.; Sheppard, L.; Yost, M.; Simpson, C., Ambient air quality measurements from a continuously moving mobile platform: Estimation of area-wide, fuel-based, mobile source emission factors using absolute principal component scores. *Atmos. Environ.* **2017**, *152*, 201-211.

37. Hsu, H.-H.; Adamkiewicz, G.; Houseman, E. A.; Zarubia, D.; Spengler, J. D.; Levy, J. I., Contributions of aircraft arrivals and departures to ultrafine particle counts near Los Angeles International Airport. *Sci. Total Environ.* **2013**, *444*, 347-355.

38. Riley, E. A.; Gould, T.; Hartin, K.; Fruin, S. A.; Simpson, C. D.; Yost, M. G.; Larson, T., Ultrafine particle size as a tracer for aircraft turbine emissions. *Atmos. Environ.* **2016**, *139*, 20-29.

39. Masiol, M.; Hopke, P.; Felton, H.; Frank, B.; Rattigan, O.; Wurth, M.; LaDuke, G., Analysis of major air pollutants and submicron particles in New York City and Long Island. *Atmos. Environ.* **2017**, *148*, 203-214.

40. Habre, R.; Zhou, H.; Eckel, S. P.; Enebish, T.; Fruin, S.; Bastain, T.; Rappaport, E.; Gilliland, F., Short-term effects of airport-associated ultrafine particle exposure on lung function and inflammation in adults with asthma. *Environ. Int.* **2018**, *118*, 48-59.

41. Riley, E. A.; Banks, L.; Fintzi, J.; Gould, T. R.; Hartin, K.; Schaal, L.; Davey, M.; Sheppard, L.; Larson, T.; Yost, M. G.; Simpson, C. D., Multi-pollutant mobile platform measurements of air pollutants adjacent to a major roadway. *Atmos. Environ.* **2014**, *98*, 492-499.

42. ASOS Network. https://mesonet.agron.iastate.edu/request/download.phtml?network=WA_ASOS. (October 17, 2019),

43. Hagler, G. S.; Yelverton, T. L.; Vedantham, R.; Hansen, A. D.; Turner, J. R., Post-processing

method to reduce noise while preserving high time resolution in aethalometer real-time black carbon data. *Aerosol and Air Quality Research* **2011**, 11 (5), 539-546.

44. Yacovitch, T. I.; Yu, Z.; Herndon, S. C.; Miake-Lye, R.; Liscinsky, D.; Knighton, W. B.; Kenney, M.; Schoonard, C.; Pringle, P., Exhaust emissions from in-use general aviation aircraft. **2016**.
45. Shirmohammadi, F.; Sowlat, M. H.; Hasheminassab, S.; Saffari, A.; Ban-Weiss, G.; Sioutas, C., Emission rates of particle number, mass and black carbon by the Los Angeles International Airport (LAX) and its impact on air quality in Los Angeles. *Atmos. Environ.* **2017**, 151, 82-93.
46. Karner, A. A.; Eisinger, D. S.; Niemeier, D. A., Near-roadway air quality: synthesizing the findings from real-world data. *Environ. Sci. Technol.* **2010**, 44 (14), 5334-5344.
47. Graham, A.; Raper, D., Transport to ground of emissions in aircraft wakes. Part I: Processes. *Atmos. Environ.* **2006**, 40 (29), 5574-5585.
48. Seinfeld, J. H.; Pandis, S. N., From air pollution to climate change. *Atmospheric Chemistry and Physics* **1998**, 1326.

Appendix

Summary of each mobile monitoring transect

N5: West Seattle (high-level) Bridge, S. Spokane St., S. Walden St., S. Horton St.

N4: SW Holden St., 1st Ave S. Bridge, S. Michigan St., S. Graham St.

N3: SW/ S. 116th St., S. Boeing Access Rd., S. Bangor St., S. Hazel St.

N2: SW/ S. 136th St., S. 135th St., S. 137th St.

N1: SW/ S. 146th St., S. 144th St.

S1: SW/ S. 200th St., S. 199th St.

S2: S. 216th St., 37th Pl S.

S3: S. 240th St.

S4: S. 272nd St., S. 277th St.

S5: SW/ S. 320th St., S. 321st St., S. 319th St.

S6 (summer only): SW 330th St., S. 336th St., Peasley Canyon Rd S.

Learn More

Web: deohs.washington.edu/mov-up

Email: elaustin@uw.edu